

AD-A153 303

AERODYNAMIC PERFORMANCE OF A WING IN GROUND EFFECT  
USING THE PANAIR PROGRAM(U) AIR FORCE INST OF TECH  
WRIGHT-PATTERSON AFB OH SCHOOL OF ENGINEERING

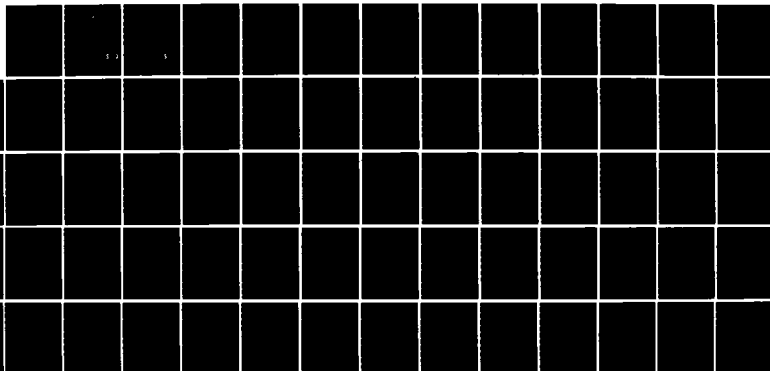
1/1

UNCLASSIFIED

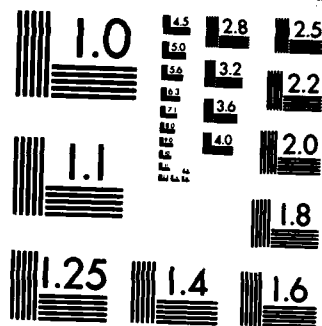
A R GOETZ DEC 84 AFIT/GAE/AA/84D-7

F/G 20/4

NL



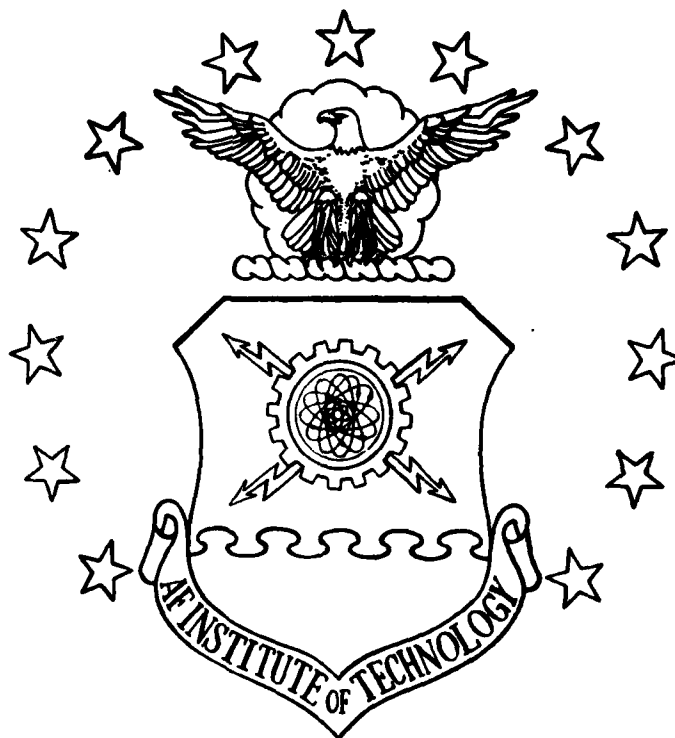
END



MICROCOPY RESOLUTION TEST CHART  
NATIONAL BUREAU OF STANDARDS-1963-A

①

AD-A153 303



AERODYNAMIC PERFORMANCE OF A WING  
IN GROUND EFFECT USING  
THE PANAIR PROGRAM

THESIS

Alfred R. Goetz

AFIT/GAE/AA/84D-7

**DISTRIBUTION STATEMENT A**

Approved for public release  
Distribution Unlimited

**DTIC**  
**ELECTE**  
**APR 30 1985**

**B**

DTIC FILE COPY

DEPARTMENT OF THE AIR FORCE  
AIR UNIVERSITY

**AIR FORCE INSTITUTE OF TECHNOLOGY**

Wright-Patterson Air Force Base, Ohio

85 4 05 042

AFIT/GAE/AA/84D-7

AERODYNAMIC PERFORMANCE OF A WING  
IN GROUND EFFECT USING  
THE PANAIR PROGRAM

THESIS

Alfred R. Goetz

AFIT/GAE/AA/84D-7

DTIC  
ELECTE  
APR 30 1985  
S B D

Approved for public release; distribution unlimited

AFIT/GAE/AA/84D-7

AERODYNAMIC PERFORMANCE OF A WING  
IN GROUND EFFECT USING  
THE PANAIR PROGRAM

THESIS

Presented to the Faculty of the School of Engineering  
of the Air Force Institute of Technology  
Air University

In Partial Fulfillment of the  
Requirements for the Degree of  
Master of Science in Aeronautical Engineering

Alfred R. Goetz

December 1984

Approved for public release; distribution unlimited

### Acknowledgements

I wish to thank the people who helped in performing this investigation and writing this thesis. I want to thank my faculty advisor, Lt Col M. L. Smith, for his guidance and assistance during the project. I also wish to thank Mr. Russell Osborn and the other personnel of the Wright Aeronautical Lab for their assistance and patience in showing me how to use PANAIR. Finally, I want to thank my family and friends for their understanding and support during the time involved in completing this thesis.

Alfred R. Goetz

Accession For	
NTIS GRA&I	<input checked="checked" type="checkbox"/>
DTIC TAB	<input type="checkbox"/>
Unannounced	<input type="checkbox"/>
Justification	
Distribution/	
Availability Codes	
Dist	Avail and/or Special
A-1	



## Table of Contents

	Page
Acknowledgements . . . . .	ii
List of Figures . . . . .	iv
List of Tables . . . . .	v
Notation . . . . .	vii
Abstract . . . . .	viii
I. Introduction . . . . .	1
II. WIG Theory . . . . .	4
III. PANAIR Method . . . . .	7
IV. Problem Definition . . . . .	10
Configuration Modeling . . . . .	10
V. Results and Discussion . . . . .	15
Wing Without Endplate Computations . . . . .	16
Wing With Endplate Computations . . . . .	18
VI. Conclusions and Recommendations . . . . .	22
Figures . . . . .	24
Appendix: WIG Configurations Examined . . . . .	51
Bibliography . . . . .	55
Vita . . . . .	56

## List of Figures

Figure	Page
1. WIG Model Geometry . . . . .	24
2. Relative Altitude Above the Ground . . . . .	25
3. Significant WIG Angles . . . . .	26
4. Possible Panel Source and Doublet Locations . . . . .	27
5. PANAIR Model Without Flap Deflection . . . . .	28
6. PANAIR Model With Flap Deflection = $15^\circ$ . . . . .	29
7. Flap Deflection Modeling Scheme . . . . .	30
8. Lift Curve Slope Without Endplates, Flap Deflection = $0^\circ$ . . . . .	31
9. L/D Comparison Without Endplates, Flap Deflection = $0^\circ$ . . . . .	32
10. $C_L$ vs. $h/\sqrt{s}$ Without Endplates, $\alpha = 0^\circ$ . . . . .	33
11. L/D vs. $h/\sqrt{s}$ Without Endplates, $\alpha = 0^\circ$ . . . . .	34
12. $C_L$ vs. $h/\sqrt{s}$ Without Endplates, $\alpha = 2^\circ$ . . . . .	35
13. L/D vs. $h/\sqrt{s}$ Without Endplates, $\alpha = 2^\circ$ . . . . .	36
14. L/D Comparison Without Endplates, Flap Deflection = $15^\circ$ . . . . .	37
15. $C_L$ vs. $h/\sqrt{s}$ Without Endplates, $\alpha = 0^\circ$ . . . . .	38
16. $C_L$ vs. $h/\sqrt{s}$ Without Endplates, $\alpha = 2^\circ$ . . . . .	39
17. $C_L$ vs. $h/\sqrt{s}$ Without Endplates, $\alpha = 4^\circ$ . . . . .	40
18. Percent L/D Error vs. $h/\sqrt{s}$ Without Endplates, Flap Deflection = $15^\circ$ . . . . .	41
19. Lift Curve Slope With Endplates, Flap Deflection = $0^\circ$ . . . . .	42

Figure	Page
20. L/D Comparison With Endplates, Flap Deflection = $0^\circ$ . .	43
21. $C_L$ vs. $h/\sqrt{s}$ With Endplates, $\alpha = 0^\circ$ . . . . .	44
22. $C_L$ vs. $h/\sqrt{s}$ With Endplates, $\alpha = 2^\circ$ . . . . .	45
23. $C_L$ vs. $h/\sqrt{s}$ With Endplates, $\alpha = 4^\circ$ . . . . .	46
24. L/D Comparison With Endplates, Flap Deflection = $5^\circ$ . . . . .	47
25. L/D Comparison With Endplates, Flap Deflection = $15^\circ$ . . . . .	48
26. Percent L/D Error vs. $h/\sqrt{s}$ With Endplates, Flap Deflection = $5^\circ$ . . . . .	49
27. Percent L/D Error vs. $h/\sqrt{s}$ With Endplates, Flap Deflection = $15^\circ$ . . . . .	50

List of Tables

Table	Page
I. Clark Y Airfoil Coordinates (Percent of Wing Chord) . . . . .	11

### Notation

AR	Aspect Ratio
b	Wing Span
c	Wing Chord
$C_D$	Drag Coefficient
$C_L$	Lift Coefficient
d	End Plate Depth
D	Drag
$D_i$	Induced Drag
h	Structural Clearance Height
L	Lift
$M_\infty$	Freestream Mach Number
q	Dynamic Pressure
s	Wing Planform Area
$\alpha$	Angle of Attack
$\beta$	$\sqrt{1 - M_\infty^2}$
$\sigma$	Prandtl's Interference Factor
$\phi$	Perturbation Potential

### Subscripts

$\infty$	Freestream
xx, yy, zz	Second Derivative with Respect to x, y and z

Abstract

*(Thesis)*  
The primary objective of this study is to correlate computed theoretical data with experimental data for wings in ground effect. This investigation uses the PANAIR *Computer program -- a* higher-order panel method to predict the lift and drag characteristics of an aspect ratio two wing, with and without endplates, operating at low speed in ground effect. The effects of altitude, trailing edge flap deflection and angle of attack are considered. Numerical results are compared with subsonic wind tunnel experimental data. For both the numerical and experimental methods, the image model technique is used to simulate ground effect. Excellent agreement between numerical results and experimental data is achieved for the wing without endplates down to low (approximately 10% ~~ten~~ percent of wing chord) altitudes. For the wing with endplates, numerical results are in good agreement with *(20%)* the experimental data for altitudes greater than approximately *(20%)* twenty percent of the wing chord. PANAIR results diverged from experimental data at lower altitudes because the model did not attempt to account for spanwise flow between the bottom of the endplate and the ground, and other viscous effects which tend to become dominant. These include a static pressure increase beneath the wing and wake distortions behind the configuration.

*Results are included: Aspect ratio 2, 10% to 100% Altitude, Lift coefficients, Lift drag ratio, Induced drag.*

AERODYNAMIC PERFORMANCE OF A  
WING IN GROUND EFFECT USING  
THE PANAIR PROGRAM

I. Introduction

This investigation attempted to determine the inviscid theory limits of PANAIR by correlating numerical lift and drag results of an aspect ratio two wing with experimental data. PANAIR (1) is a higher-order paneling program designed to predict flows about arbitrary configurations.

The wing configuration selected for modeling is based on the availability of experimental data for which a comparison can be made with theory. A wind tunnel examination of the effects of various wing endplate and camber changes on the aerodynamic characteristics of low aspect ratio wings in ground effect (2) is used as the basis for the experimental portion of the investigation.

Figure 1 illustrates the wing-in-ground effect (WIG) configuration modeled. The WIG model consists of an 11.7 percent thick, constant section, aspect ratio 2.0, rectangular planform wing with endplates and a trailing edge flap hinged at the 75 percent wing chord position. Figure 2 shows the relative heights above the ground where the PANAIR lift coefficient and lift/drag ratio computations are made. The altitude parameter,  $h/\sqrt{s}$ , is measured as a fraction of the wing chord. Additional calculations are made with and without the endplate at  $h/\sqrt{s} = 3.0$  and 5.0 to obtain out of ground effect reference data.

Several parameters are varied during the course of the study. The parameter variations are dictated by the variations made in the wind tunnel investigation. Parameter variations examined are angle of attack, flap deflection, altitude, and endplate presence or absence. Additionally, several computations are made with and without the endplate for different aspect ratio wings to compare the computed lift curve slope with the experimental slope.

The PANAIR production code is used in the computation of the WIG lift and drag characteristics since recent Flight Dynamics Laboratory experience with the code (3) indicated that this method might have the versatility to handle the WIG aerodynamic prediction problem. It was expected that the inviscid theory used in PANAIR would not give accurate results when viscous effects on the WIG configuration were significant.

The results obtained through this investigation indicate that PANAIR can be used without WIG model modifications for aerodynamic characteristic predictions dependent on the specific configuration. Endplate and flap deflection numerical results indicate that modifications have to be made to the WIG model to incorporate viscous effects encountered when flaps and endplates are used. For the aspect ratio two wing without endplates, the results show good data correlation between theory and experiment down to an  $h/\sqrt{s}$  value of 0.04. The addition of endplates significantly affects the lift coefficient and lift/drag (L/D) ratio data correlation between PANAIR and experimental data. PANAIR satisfactorily predicts L/D values down to  $h/\sqrt{s} = .08$  at zero degrees angle of attack. As the angle of attack is increased, the

PANAIR method underpredicts L/D improvement near the ground by as much as 33 percent at four degrees angle of attack. This level of error is unacceptable for performance estimation purposes.

Results with a trailing edge flap deflection follow similar trends to the results obtained for the basic wing with endplates. Lift and L/D calculations are significantly lower as the ground is approached than the experimental values. Also, for the flap deflection cases at  $h/\sqrt{s} = 0.32$ , the highest ground effect altitude at which calculations are made, L/D predictions show considerably more error than similar  $h/\sqrt{s}$  cases without a flap deflection.

Analysis of these results indicates that WIG analytical model modifications must be made to account for the viscous effects encountered at very low altitudes. Modeling modifications to incorporate wake distortion and endplate vortices are not examined during this initial investigation, but should be considered in any follow-on efforts.

## II. WIG Theory

The aerodynamic characteristics of wings operating at very low altitudes has long interested investigators in search of efficient modes of travel. A wing is considered to be in "ground effect" when it is operating at altitudes on the order of its chord length (4). Unfortunately, the development of WIG vehicle concepts requires the solution of some very difficult engineering problems. The majority of investigations conducted on the aerodynamic characteristics of wings operating in ground effect are related primarily to take-off and landing of conventional aircraft. However, some studies have been directed towards development of dedicated WIG air vehicle concepts. The development of an accurate procedure for theoretically predicting the aerodynamic forces on lifting surfaces operating near the ground would be very useful in designing WIG-type vehicles.

A wing operating at ground effect altitudes experiences an increase in aerodynamic lift and reduced drag, and hence a higher lift/drag ratio than an out-of-ground effect (OGE) wing. The basic principles involved can be explained by using the concept of a "mirror image" wing which is a reflection of the real wing in the ground plane. The wing and its image can be replaced by distributions of sources and vortices. The sources representing the displacement flow of the image wing produce an upwash over the front part of the physical wing and a downwash over the rear part of the wing. To counteract this, a vortex distribution is required which alters the effective camber of the wing. The effective camber is increased because of the circulation around the image wing, and is equivalent to an increase in effective angle of attack.

The trailing vortices of a wing of finite span are also reflected in the ground plane. These image vortices induce an upwash at the physical wing so that the induced angle of attack is reduced as compared to the free stream condition, reducing the induced drag. Jones (5) shows that the reduction in induced drag due to ground effect is:

$$\Delta D_i = \frac{\sigma L^2}{\pi q b^2} \quad (1)$$

where  $\sigma$  is Prandtl's interference factor and depends on the distance between the real and image wings.

Figure 3 shows the angles involved. When a wing is flying at the same geometric angle of attack, near the ground the induced angle of attack is less and the effective angle is greater. The lift is greater and the drag is less, causing an increase in the lift/drag (L/D) ratio.

An additional improvement in L/D is possible by the use of endplates on WIG configurations (6). In most WIG applications, the endplates serve two functions: the containment of a high pressure air "bubble" under the wing and air vehicle support at static and low forward speed conditions, allowing greater clearance heights between the aircraft structure and the ground.

Early investigators in the WIG field of study (7, 8) developed theories and attempted to show correlation between theory and wind tunnel data. Other contributors since then have expanded and increased the amount of knowledge in this area, but precise correlation between

experiment and theory was not completely achieved. Computational paneling methods have the potential to, if not completely solve the WIG aerodynamic prediction problem, at least extend the limits to which inviscid flow theory can be used.

### III. PANAIR Method

PANAIR is a higher-order paneling method which solves the Prandtl-Glauert equation for incompressible flows in both the subsonic and supersonic flow regimes:

$$\beta^2 \phi_{xx} + \phi_{yy} + \phi_{zz} = 0 \quad (2)$$

The solution is obtained numerically by approximating the configuration surface with a set of quadrilateral panels on which unknown singularity strengths are defined. Each panel is defined by its four corner points, with each point's x, y and z coordinates given in the same arbitrary coordinate system. A network consists of a grid of panel corner points, and does not need to lie in a plane. Source and doublet distributions are defined on the surface for each network. The source and doublet distributions can be of the "null", "analysis" or "design" type. A "null" type distribution means the singularity distribution is zero over the entire network. An "analysis" singularity distribution (used in this WIG investigation) uses the zero normal mass flux boundary condition for a modeled configuration surface. Figure 4 shows the possible source and doublet locations for an "analysis" singularity distribution. A "design" distribution is used when the boundary conditions correspond to specifying a pressure distribution on the surface. Wake networks generally use only doublet distributions to model a wake surface and are usually attached to the trailing edge of a lifting surface.

For all of the networks, boundary conditions are imposed at a discrete set of points (control points), thereby generating a system of

linear equations relating the singularity strengths to the boundary conditions. Control points are located at either the panel center, near the midpoint of a panel edge if it lies on a network edge, or near a panel corner that lies on a network edge. For "analysis" networks, source distributions are located only at panel centers. Doublet distributions are located at panel centers and along network edges as necessary, depending on control point location. Doublets are required at network edges because of the quadratic variation of the doublet strength approximation. A quadratic variation causes rapid changes in doublet strength. Extrapolating the doublet strength from the interior of the network to the edges would not be advisable because of these rapid changes. Since the source strength is only linear, similar problems do not occur in the source distribution. Once the source and doublet strengths are numerically established, the properties of the flow are determined.

Higher-order panel methods, such as PANAIR, have emerged in recent years as a response to limitations uncovered in earlier, low order methods. In the lower order panel methods, the singularity strengths were generally constant, or varied only in one direction, over each panel. This resulted in discontinuities in singularity strengths between panels which made the sensitivity of the solution dependent on panel spacing or density. The solution sensitivity made successful lower order computations dependent on the skill of the individual user. These sensitivities to paneling density and distribution have been largely overcome with PANAIR in which singularity strengths vary in a more continuous manner over the panels. As previously noted, PANAIR

uses a linear source variation and a quadratic doublet variation. A doublet distribution whose order is one higher than that of the source distribution is the next higher order approximation to use above constant source and doublet strengths. A higher order doublet distribution also provides a continuous doublet distribution. A detailed discussion of the justifications for the higher order approximation is given in (1).

Flight Dynamics Laboratory out-of-ground effect aerodynamic predictions (3, 7, 8) on a variety of complex aircraft configurations, using PANAIR, have produced excellent theory to experiment correlations. However, applicability of the potential flow PANAIR code to WIG aerodynamic prediction may be more restrictive because viscous flow effects tend to dominate WIG aerodynamic force generation. This is particularly true at extremely low altitudes, when the wing endplate and ground form a narrow slot through which spanwise flow, produced by high pressure air under the wing, must pass.

#### IV. Problem Definition

The specific area of interest for this investigation is modeling a low aspect ratio wing with endplates operating in ground effect, and determining the limitations of the PANAIR inviscid flow solution in predicting the aerodynamic characteristics of this configuration. This study is intended to be an initial examination of this configuration. The results of this investigation indicate where difficulties still remain in applying PANAIR to WIG configurations. These problems must be addressed in future applications in order to accurately predict the aerodynamic characteristics of WIG vehicles.

##### Configuration Modeling

The numerical models used in this study simulated low aspect ratio wings with an 11.7 percent thick Clark Y airfoil section. The wing planforms are rectangular with aspect ratios of 1.0, 2.0 and 4.0. Flap deflections of 0.0, 5.0 and 15.0 degrees are used during the course of the computations. Three angles of attack are run: 0.0, 2.0 and 4.0 degrees. The specific configurations examined are tabulated in the appendix. The central configuration studies is an aspect ratio two wing with a flap and endplate.

Table I shows the airfoil station coordinates for an 11.7 percent thick Clark Y airfoil. Additional stations are necessary in order to properly model the airfoil. To obtain the additional points, the coordinates of the given stations up to the 10 percent chord point are plotted and the leading edge profile then added. The additional points are interpolated graphically from the profile. The extra station

TABLE I

## Clark Y Airfoil Coordinates (Percent of Wing Chord)

<u>Station</u>	<u>Upper</u>	<u>Lower</u>
0.0	3.50	3.50
0.0 *	3.60	3.40
0.2 *	4.15	2.75
0.625 *	4.80	2.50
1.25	5.45	1.93
2.50	6.50	1.47
3.60 *	7.22	1.23
5.0	7.90	0.93
7.5	8.85	0.63
10.0	9.60	0.42
15.0	10.68	0.15
20.0	11.36	0.03
30.0	11.70	0.00
40.0	11.40	0.00
50.0	10.52	0.00
60.0	9.15	0.00
70.0	7.36	0.00
75.0 *	6.25	0.00
80.0	5.22	0.00
85.0 *	4.00	0.00
90.0	2.80	0.00
95.0	1.49	0.00
100.0	0.12	0.00

\* = added station

coordinates not only make the numerical profile more continuous, they also provide the proper geometry for PANAIR by making all panels quadrilateral (a necessary condition unless special precautions are taken).

The overall PANAIR numerical models used for the WIG calculations are shown in Figures 5 and 6. Figure 5 shows the configuration with no flap deflection and Figure 6 shows a 15 degree flap deflection. The models consist of source and doublet networks on the upper and lower wing surface, upper and lower flap surface, the trailing edge and the endplates. Wakes are modeled by flat doublet networks extending downstream from both the wing and endplate trailing edges parallel to the ground for 50 chord lengths. The trailing edge of the flap does not come to a point, so wakes have to be extended from the upper, lower and side edges of the flap's trailing edge. The endplate is modeled so that its bottom is always parallel to the flow regardless of the wing's angle of attack. This geometry corresponds to that used during the WIG wind tunnel test (2). The altitude parameter  $h/\sqrt{s}$  is measured from the bottom edge of the endplate (cases with endplates) or the wing trailing edge (cases without endplates). This difference in measurement is due to the fact that  $h$  is defined as the minimum structural clearance height from the ground plane (2).

The spanwise panel distribution used on the models is selected on the basis of discussions with Flight Dynamics Laboratory personnel who had previous experience with PANAIR in making out of ground effect calculations with wing alone and wing/body configurations. Starting at the wing centerline, chordwise stations are located at each 20

percent span position out to 0.6 semi-span. From the 0.6 position outboard to the wingtip, chord stations are located at every 10 percent of the semi-span. This panel distribution increases the panel density at the wingtip, providing better resolution at the wingtip region where greater flow field changes are occurring. A total of 357 quadrilateral panels in 6 networks are used to define the wing semi-span surface which is used to make the aerodynamic calculations. An additional network containing 40 panels is used to define the endplate for cases with an endplate.

Modeling the flap deflection is accomplished by placing the pivot point of the flap at the 75 percent chord point on the wing lower surface. Figure 7 shows the flap deflection modeling scheme. The profile of the flap is maintained for all flap deflections. A single panel adjustment is required between the wing-top and flap-top networks to assure that no gaps occur between the two networks. For each flap deflection the endplate network is modified to insure abutment between the endplate and the lower surface of the flap.

Ground effect is simulated by the image technique. A similar model is positioned opposite to the primary computational model with the plane of symmetry representing the ground position. The image technique was also used for the WIG wind tunnel test.

Modeling the WIG configuration presents problems unique to this type of configuration. Each angle of attack, flap deflection, height and endplate configuration produces a unique set of points defining the model. On many non-WIG models, the angle of attack is inputted and PANAIR handles the network model orientation. For this WIG

configuration, the requirement that the bottom of the endplate be parallel to the flow indicates a more involved approach. The modeled networks must be rotated to the proper angle of attack prior to inputting the points into PANAIR. This requires a recalculation of all panel coordinates to their proper orientation. The angle of attack then inputted to PANAIR is 0 degrees, but the WIG model is actually at a specified angle to the flow. Compounding the angle of attack problem is incorporating the flap deflection and placing the configuration at the proper altitude. A computer program was written to incorporate the various parameter changes. Aspect ratio, angle of attack, flap deflection, altitude and endplate option are inputted, and the program orients the selected configuration to the proper angle of attack and altitude, and produces a data file for input into PANAIR. This different approach for WIG models should be a consideration in any future study efforts. Results of this study indicate that modifications to standard panel modeling procedures may be necessary for some WIG configurations.

## V. Results and Discussion

The primary purpose of this investigation is the correlation of computed aerodynamic data versus experimental results for a low aspect ratio WIG configuration. The most significant parameter examined in the wind tunnel test was the lift/drag (L/D) ratio, which is a measure of efficiency. The test variables were selected to gain some understanding of the effects of endplates and flap deflection of L/D. This computational study duplicated the parameter variations to determine the numerical results for the same configurations.

The numerical PANAIR L/D results could not be directly compared to the experimental data due to the fact that PANAIR is an inviscid solution code. When computing the drag coefficient, PANAIR does not incorporate form drag. Thus the total drag coefficient to use in L/D calculations is:

$$C_D = C_{D0} + C_{D \text{ PANAIR}} \quad (3)$$

The value of  $C_{D0}$  is determined from  $C_L$  versus  $C_D$  plots for the aspect ratio two wing out of ground effect with and without endplates. The plots are presented in the wind tunnel test report (2). For the wing without endplates,  $C_{D0} = 0.01$ . With endplates,  $C_{D0} = 0.011$ . These values are incorporated into the calculations to determine the PANAIR results.

The altitude parameter  $h/\sqrt{s}$  is presented in the wind tunnel test report for design considerations (2). As previously noted,  $h$  is the minimum structural clearance height and  $s$  is the total wing area. The

report assumed that a wing area and altitude would be predetermined by design conditions.

The numerical computations for this investigation are run at a Mach number of  $M = 0.30$ . This Mach number corresponds to the Reynolds number of  $2.55 \times 10^6$  (based on wing chord) used for the wind tunnel tests.

#### Wing Without Endplate Computations

Aerodynamic calculations are initially performed on the aspect ratio two wing without endplates as a check case. PANAIR calculations on other wing and wing/body geometries had produced excellent theory to experiment correlation for out-of-ground effect cases (3, 9, 10). However, the usefulness of this method for in-ground-effect predictions was unknown. Some basic limits of applicability needed to be established for a relatively simple case prior to examining the more complex configuration of a wing with endplates and flap deflection.

No Flap Deflection. Figure 8 shows the lift coefficient versus angle of attack for different aspect ratio wings without endplates. The flap is not deflected for these cases and the wings are out of ground effect. It can be seen that the PANAIR results show a fairly good correlation with the experimental data, especially for the aspect ratio four wing. For the primary configuration (aspect ratio two), the difference in lift curve slope is approximately 5 percent. These calculations are useful in indicating an approximate accuracy estimation for the PANAIR results.

Figure 9 is a comparison of theoretical and experimental L/D values for the aspect ratio two wing without endplates and zero flap

deflection as a function of wing altitude above the ground. The results show good theory to experiment data correlation down to an  $h/\sqrt{s}$  value of 0.04. Problems begin to occur in this region and are believed to be caused by the close proximity of the actual and image model wakes. Similar trends toward underprediction of L/D gain as the ground is approached are noted at both zero and two degrees angle of attack.

Examining the L/D and  $C_L$  variation with altitude at a given angle of attack is also useful in assessing the accuracy of the computed results. Figures 10 through 13 present both theoretical and experimental L/D and  $C_L$  results for zero and two degrees angle of attack. The data shown in these figures along with Figure 9 show that PANAIR does very well for the wing without endplates or flap deflection.

With Flap Deflection. Additional calculations are made on the wing without endplates to determine what effect flap deflection would have on the numerical results. This is done in an attempt to separate the effects of the flap and endplate on the computations. The effects of each could then be observed.

Figure 14 shows the theoretical and experimental L/D versus  $C_L$  values for the aspect ratio two wing without endplates and a 15 degree flap deflection. It can be seen that as the ground is approached, the theoretical results begin to deviate from experiment. Close to the ground, PANAIR underpredicts both lift and drag on the wing. The lift coefficient underprediction is believed to be caused by the pressure build-up which occurs under the wing by the deflected flap "trapping" the air. Figures 15 through 17 indicate the underprediction of  $C_L$ .

The differences in drag coefficient are believed to stem from the wake model used. The model wakes extend from the trailing edge of the flap parallel to the ground. Initially extending the wakes at the same angle as the flap deflection and then turning the wakes parallel to the ground may improve the computational results. Close to the ground, however, problems may occur regarding the clearance between the model and image wakes. (A modified wake model could not be incorporated into the calculations due to time constraints.) As an aid in determining when model modifications may be necessary, Figure 18 shows the percentage of error in L/D versus  $h/\sqrt{s}$  for the data of Figure 14.

#### Wing With Endplate Computations

A wing with endplates is the classical WIG configuration that has been tested on many prototype vehicles. The endplate used in this study has a depth ratio ( $d/c$ ) of 0.10. The depth of the endplate  $d$  is measured from the trailing edge of the wing with no flap deflection and is indicated in Figure 1. The endplate serves to restrict the spanwise flow below the wing, and is the only aerodynamic difference between the wing with endplates and the aspect ratio two wing alone which was previously discussed. This difference did, however, significantly affect the PANAIR/experiment lift coefficient and L/D data correlation.

No Flap Deflection. For the wing with endplates, the initial calculations are again made to examine the lift curve slope for different aspect ratios out of ground effect. Figure 19 shows the theoretical/experimental data comparison. The theoretical results deviate to a much greater extent than for the wing alone. These results

are an immediate indicator that a much greater error should be expected in the ground effect calculations involving the endplate. The data differences appear to have a dependence on angle of attack. At zero degrees, the computational results compare favorably with the experimental data. As the angle of attack increases, the computed values deviate, leading to large errors in the lift curve slope. The wake model changes noted previously would probably improve the computational results, but additional effects from the endplates must be considered. During this investigation, related studies were discovered which indicated that an additional lateral distortion of the wing wake between the endplates occurs (11), and vortices are present outside the endplates (12). Again due to time constraints, these model improvements could not be incorporated in this initial investigation.

Figure 20 compares PANAIR and experimental results for the wing model with endplates but no flap deflection. As the data shows, PANAIR predicts  $L/D$  values reasonably well down to an  $h/\sqrt{s}$  value of 0.08 at zero degrees angle of attack. As the angle of attack is increased, however, the PANAIR method underpredicts  $L/D$  improvement near the ground by as much as 33 percent at four degrees angle of attack and  $h/\sqrt{s} = 0.04$ . This level of error is unsatisfactory when attempting to estimate vehicle performance, and the reasons for its occurrence require examination.

Plotting  $C_L$  versus  $h/\sqrt{s}$  for the endplate configured wing again provides an indication of the problem. Figures 21 through 23 show the comparison of these values. As shown, the lift predictions made using PANAIR deviate considerably from the measured data at increasing angle

of attack and as the ground is approached. An explanation for this difference is the inability of the PANAIR code to handle the wing with endplate problem without appropriately modeling the jet-like slot flow issuing from between the bottom of the endplate and the ground. The velocity of this jet gets stronger as the ground is approached because of the build-up in static pressure under the wing. This leakage flow separates from the bottom of the endplate and rolls up into a vortex some distance downstream from the wing. These additional vortices (one at each wing tip) are not accounted for in the numerical model, and depending on vortex strength, could be a contributing factor for the significant underprediction of lift and drag near the ground.

With Flap Deflection. The addition of flap deflection to the wing with endplates provides the most complex configuration examined in this study. It could thus be expected that considerable error might occur in the calculations. PANAIR aerodynamic calculations for the aspect ratio two wing with endplates and flap deflections of 5 and 15 degrees are presented in Figures 24 and 25 respectively, compared with the experimental data. The trends of the theoretical results for both flap deflections follow that obtained for the basic wing with endplates in that lift and L/D are underpredicted as the ground is approached. The problem of two troublesome parameters (endplates and flap deflection) serves to worsen the amount of error. The L/D error with endplates, 15 degree flap deflection, four degrees angle of attack and  $h/\sqrt{s} = 0.04$  is 38 percent, versus 31 percent for the same configuration minus the endplate, and 33 percent with the endplate but without a flap deflection. Figures 26 and 27 show the percentage of L/D error

versus  $h/\sqrt{s}$  for the two flap deflections. Comparison of the two figures shows the increase in error as the flap deflection increases. The flap deflection contributes to the wake distortions behind the configuration. It becomes evident that wake distortion and endplate vortex effects must be incorporated into the modeling scheme if the accuracy of the PANAIR results is to be improved.

## VI. Conclusions and Recommendations

PANAIR calculations of lift coefficient and L/D ratio for an aspect ratio two wing without endplates operating in ground effect compare favorably with experimental results down to a ground height of approximately  $h/\sqrt{s} = 0.04$ . However, the addition of flap deflection and/or endplates must be handled by modifications to the numerical model. When endplates are added, PANAIR aerodynamic estimates begin to diverge from experimental results at a ground height of  $h/\sqrt{s} = 0.08$  (a wing height of approximately 20 percent wing chord). Flap deflection causes additional error in the computational results. The discrepancies between theory and experiment are believed to be caused in part by not modeling the jet flow between the endplates and ground plane and the wake displacements which occur. In addition, lift underprediction by PANAIR for a wing with endplates can be associated with the higher pressure air "bubble" that occurs and is not accounted for in the inviscid numerical solution. More accurate theoretical results may be achieved by revising the PANAIR modeling scheme to include wake distortion and vortex effects. Care must be taken concerning angle of attack and wake network clearance when modeling WIG configurations for PANAIR to avoid numerical errors from those sources.

It is recommended that any future efforts attempt to remedy the modeling deficiencies revealed in this initial study. Improved wake and jet flow models may provide greater accuracy for the PANAIR method. The wake models should incorporate the physical distortions that occur behind the WIG configuration. These include lateral distortions and wake angle off of the WIG trailing edge due to angle of

attack and/or flap deflection. Modeling the jet flow issuing from beneath the endplate may be accomplished by incorporating an additional network into the WIG modeling scheme. The jet flow rolls up into a vortex behind the endplate (12), and adding a vortex-shaped network could be an initial step in accounting for the flow effects experimentally observed.

Other parameters not examined in this analysis such as WIG stability and aerodynamic moments may also be compared with experimental data. Additional comparisons could be made regarding the image technique solution versus numerically modeling the physical ground plane. Although PANAIR is generally considered more insensitive to paneling density and distribution, this assumption may not be correct at ground effect altitudes. Comparison of different paneling schemes should be examined to determine the validity of PANAIR insensitivity for WIG configurations. Modeling schemes which are accurate for relatively simple configurations might then be applied to more complex WIG vehicles for aerodynamic prediction accuracy. Much investigation and study in this area remains before numerical WIG vehicle modeling can be applied with confidence.

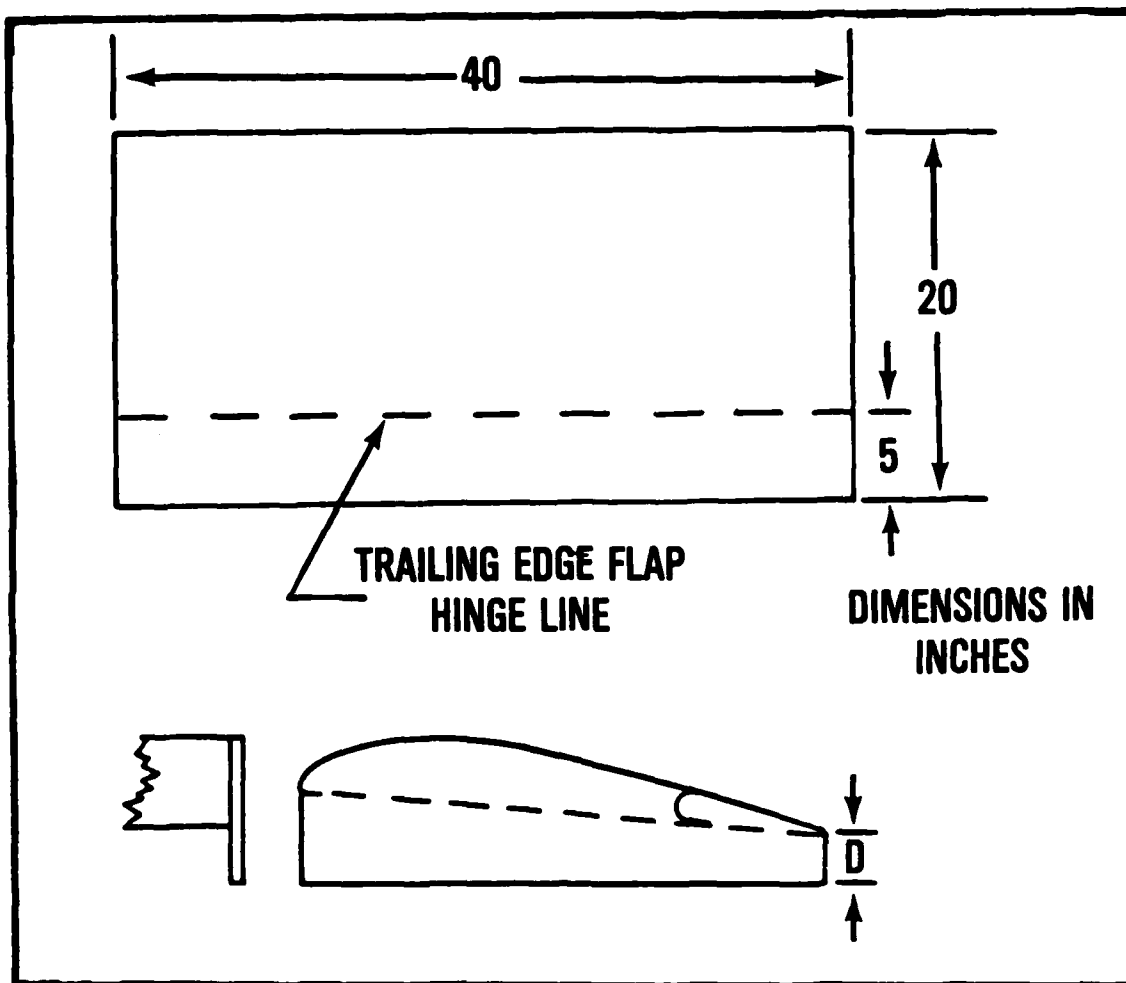


Figure 1. WIG Model Geometry

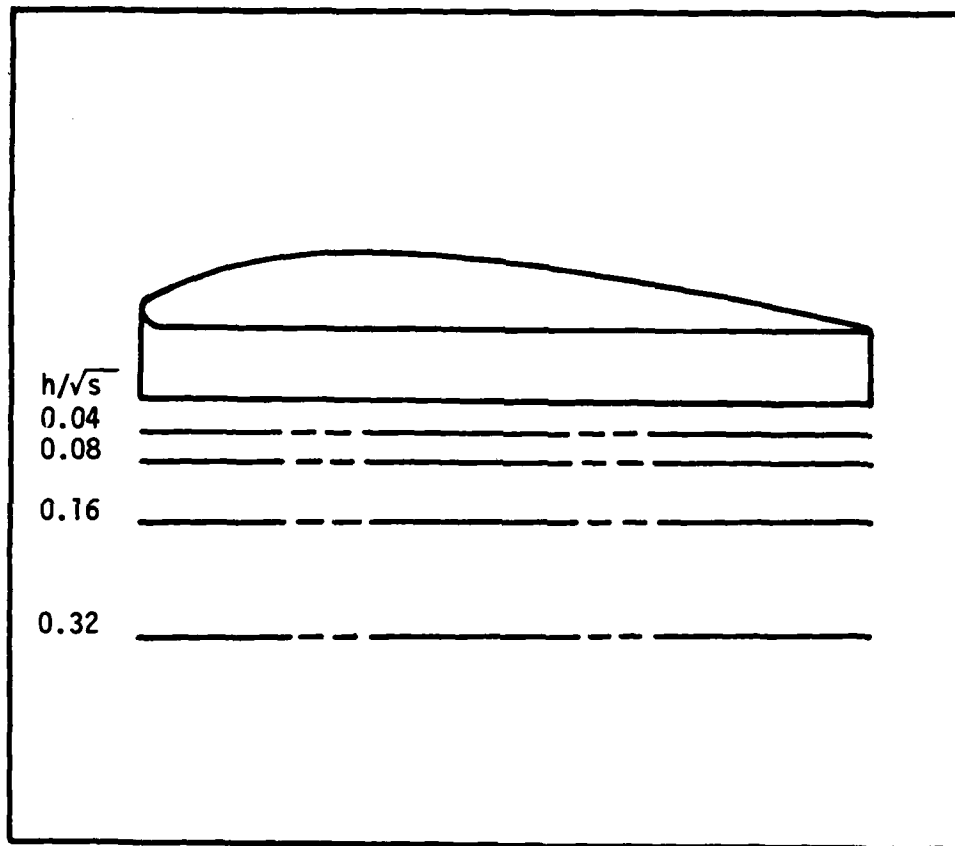


Figure 2. Relative Altitude Above the Ground

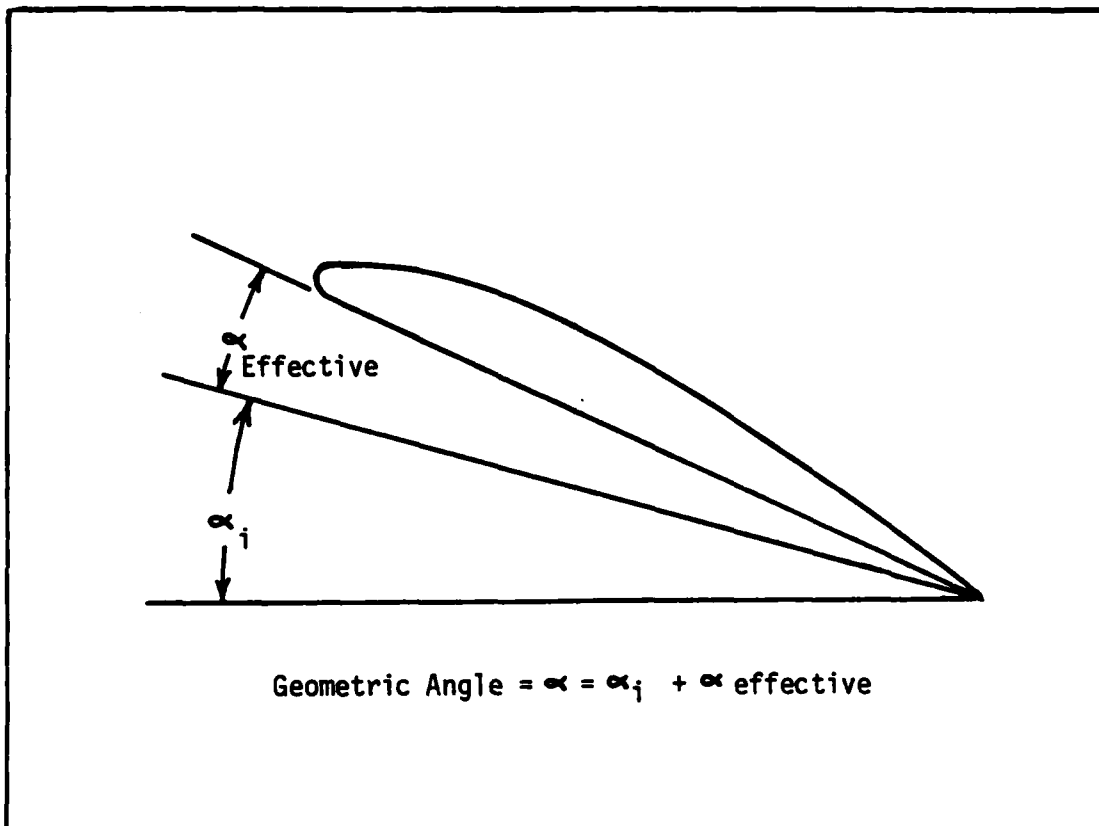


Figure 3. Significant WIG Angles

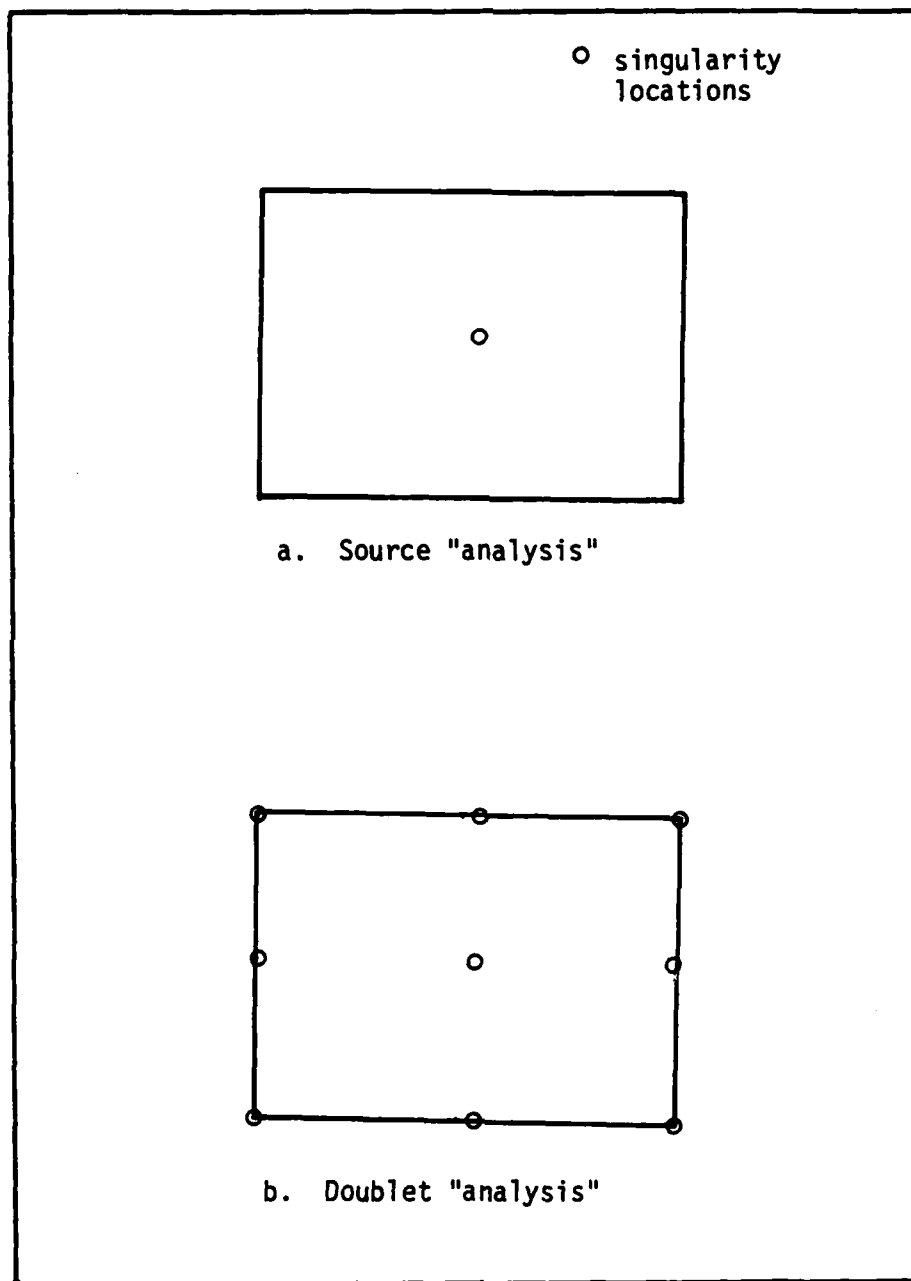


Figure 4. Possible Panel Source and Doublet Locations

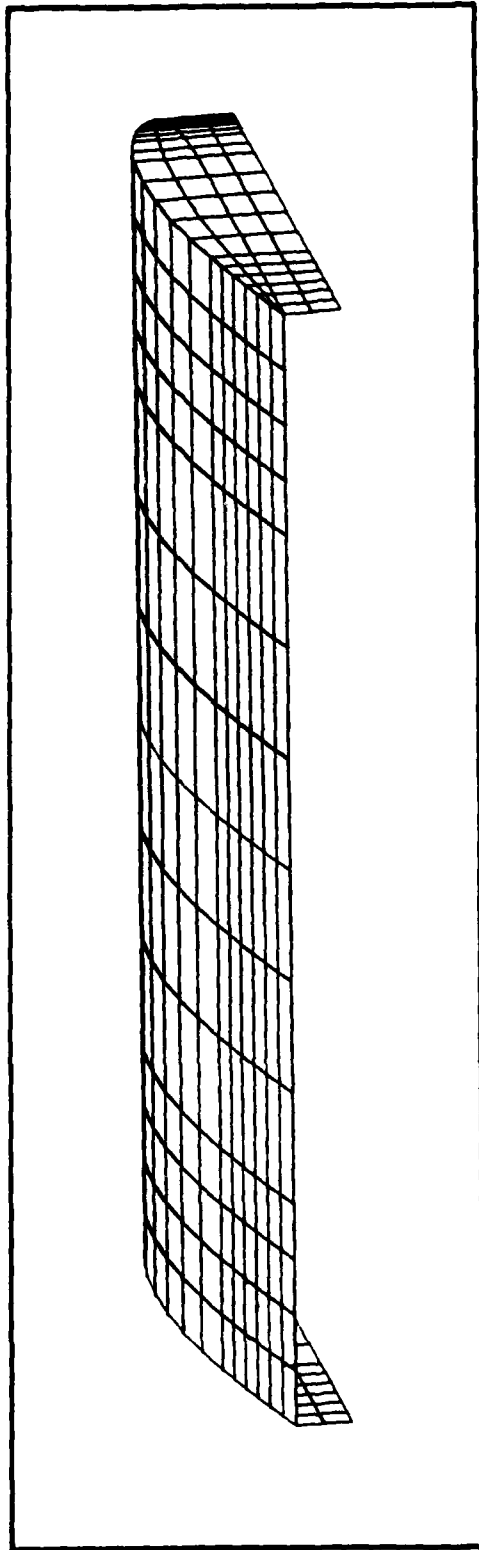


Figure 5. PANAIR Model Without Flap Deflection

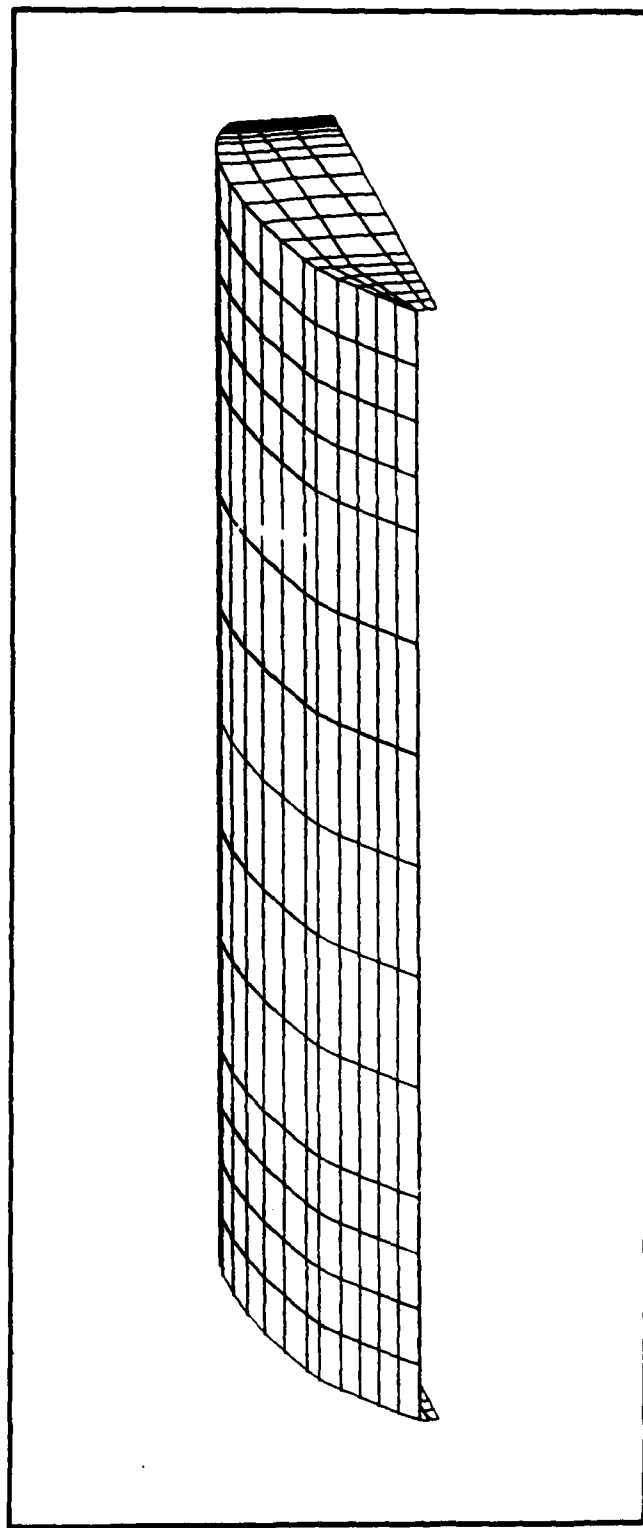


Figure 6. PANAIR Model With Flap Deflection =  $15^\circ$

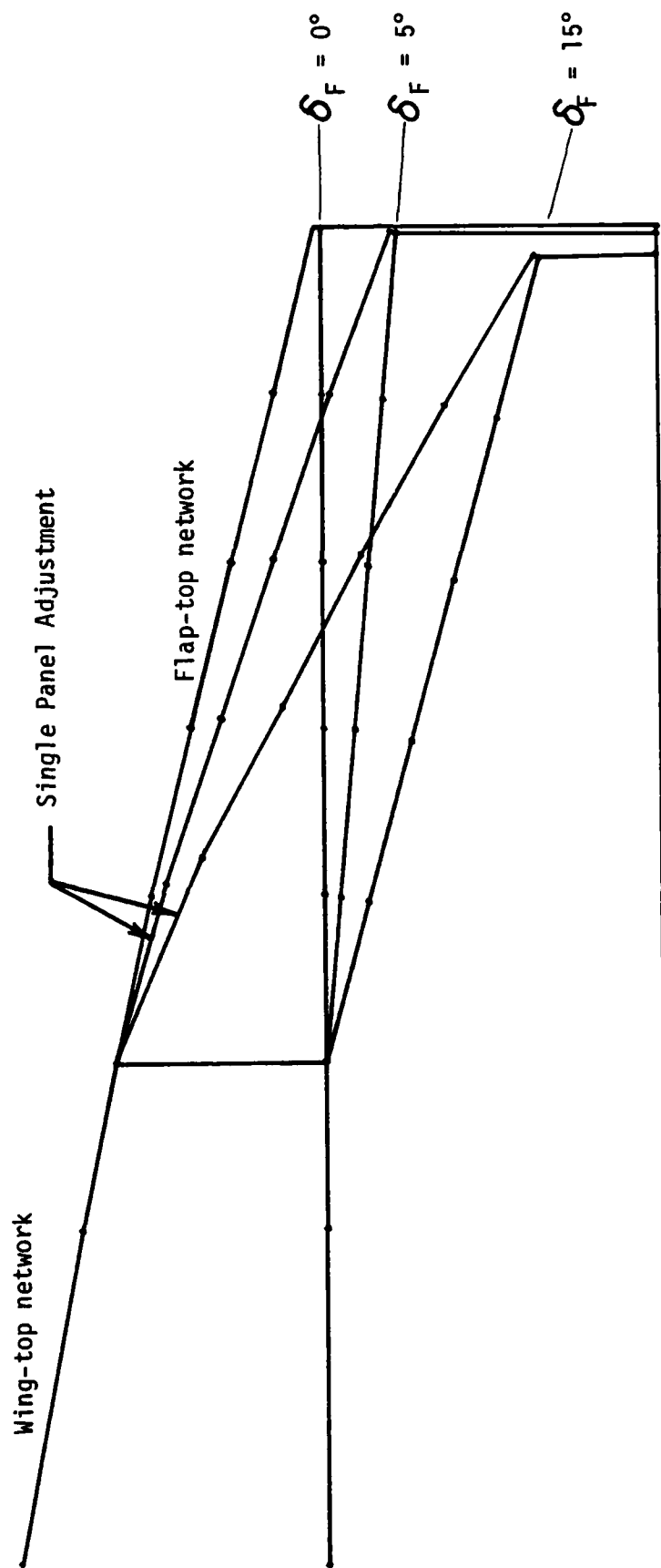


Figure 7. Flap Deflection Modeling Scheme

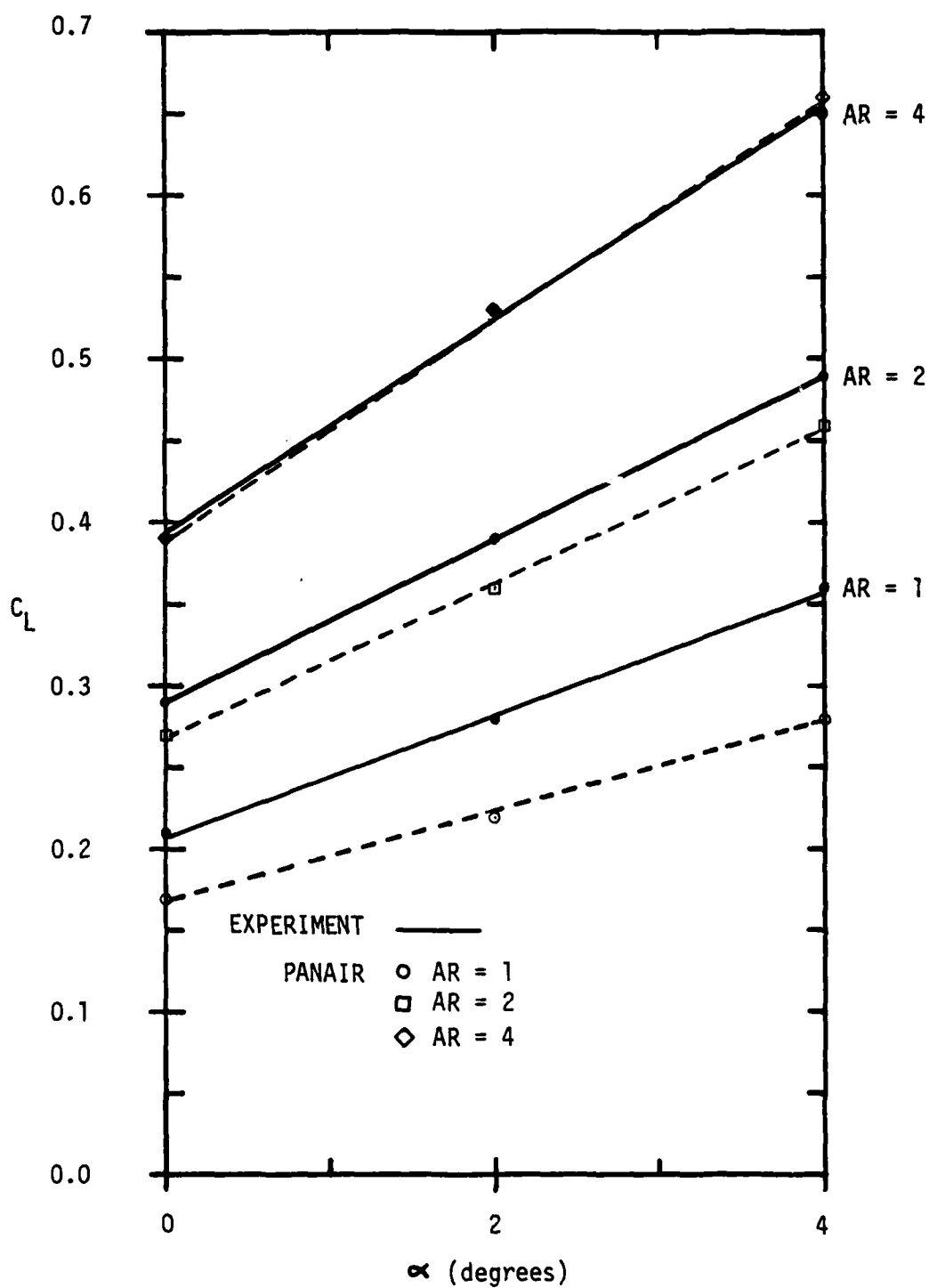


Figure 8. Lift Curve Slope Without Endplates,  
Flap Deflection =  $0^\circ$

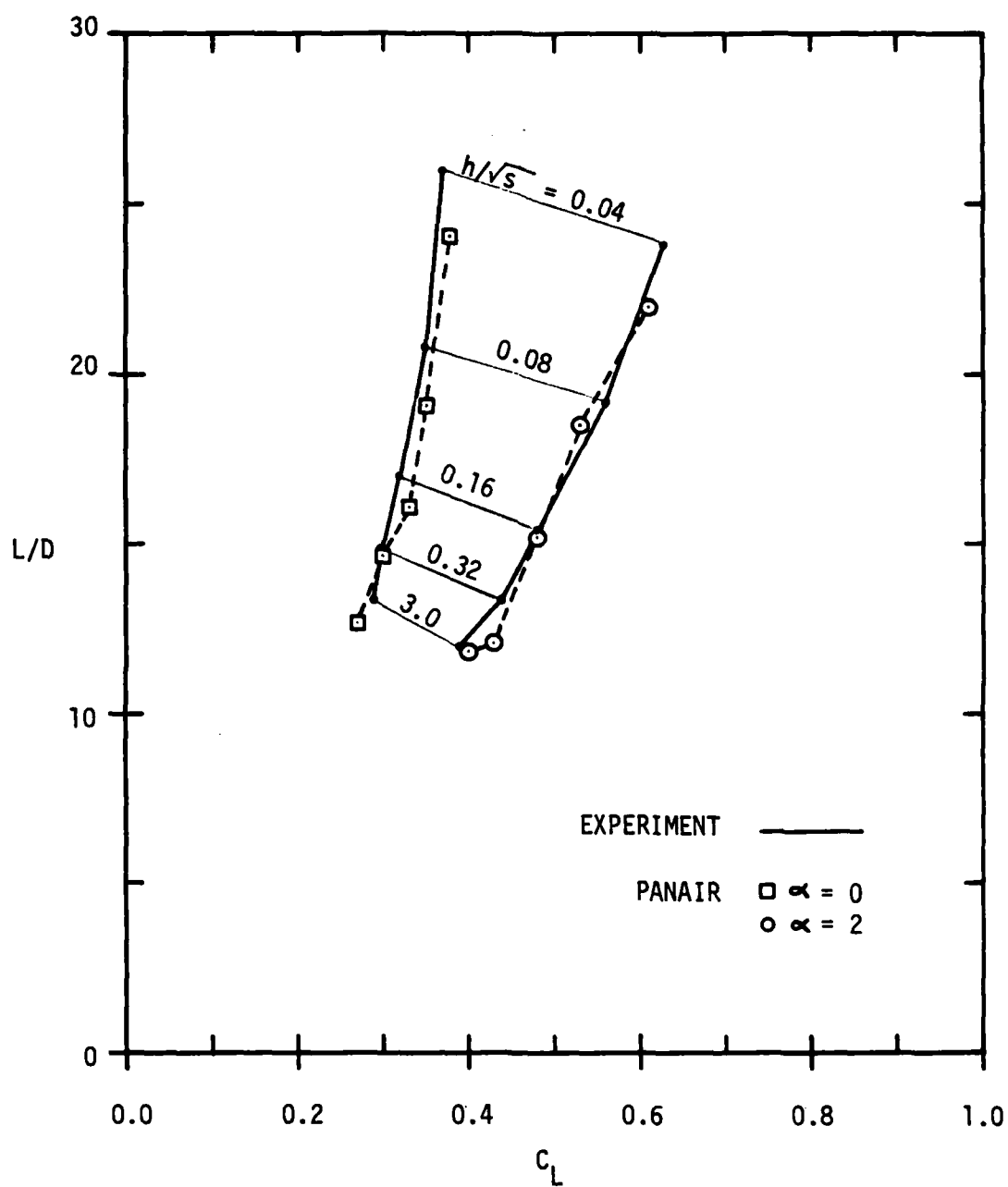


Figure 9.  $L/D$  Comparison Without Endplates,  
Flap Deflection =  $0^\circ$

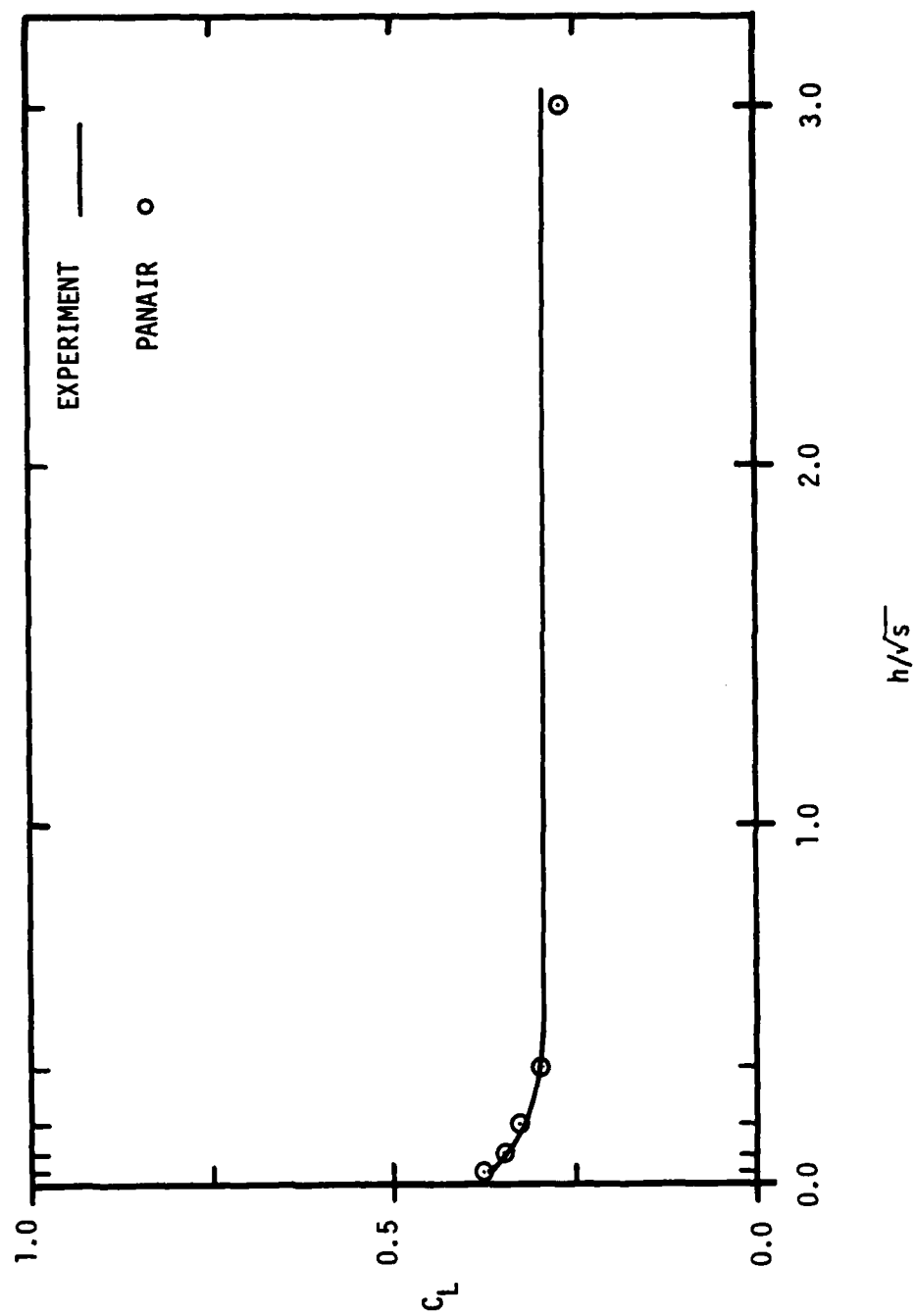


Figure 10.  $C_L$  vs  $h/\sqrt{s}$  Without Endplates,  $\alpha = 0^\circ$

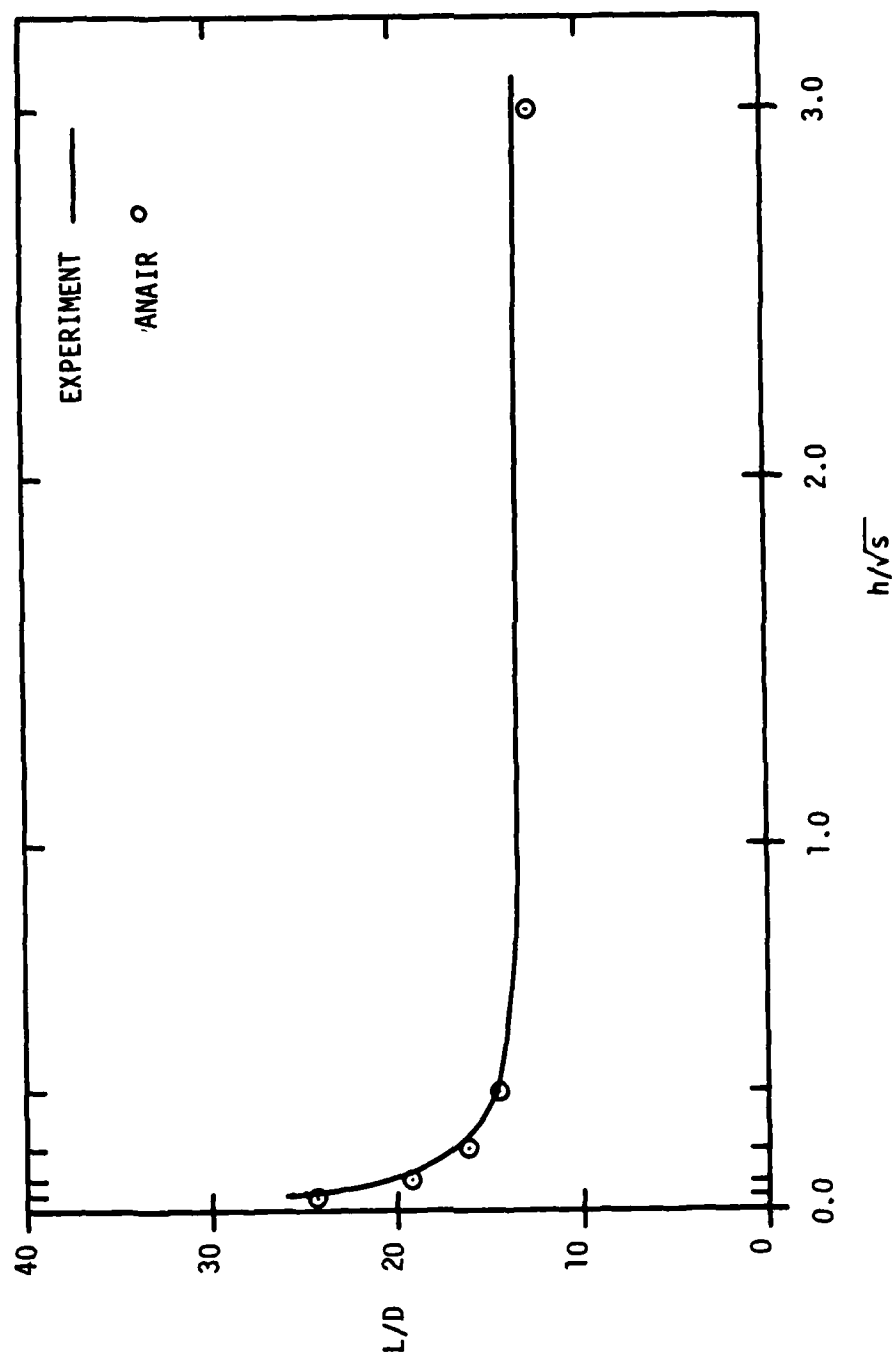


Figure 11.  $L/D$  vs  $h/\sqrt{s}$  Without Endplates,  $\alpha = 0^\circ$

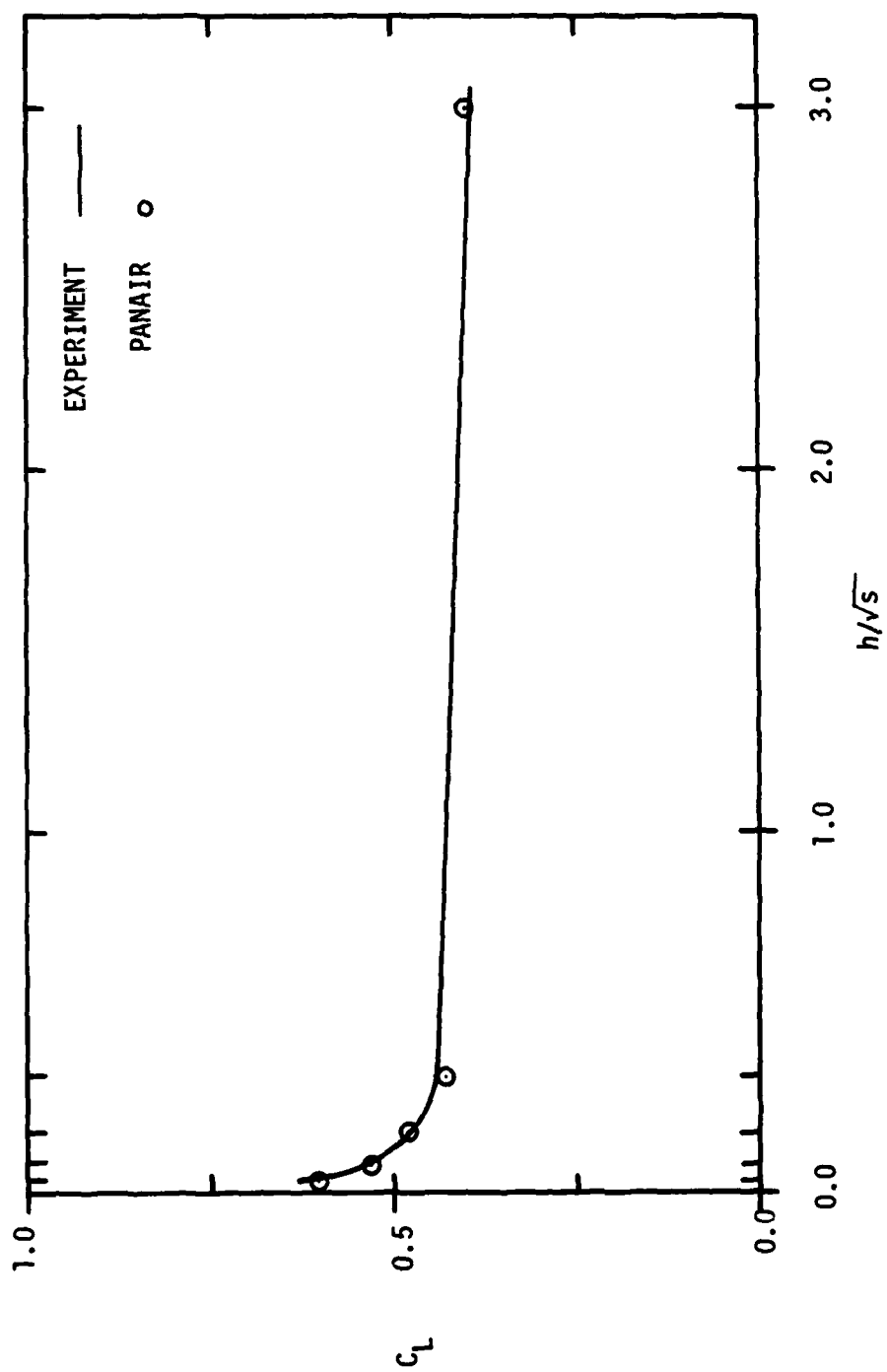


Figure 12.  $C_L$  vs  $h/\sqrt{s}$  Without Endplates,  $\alpha = 2^\circ$

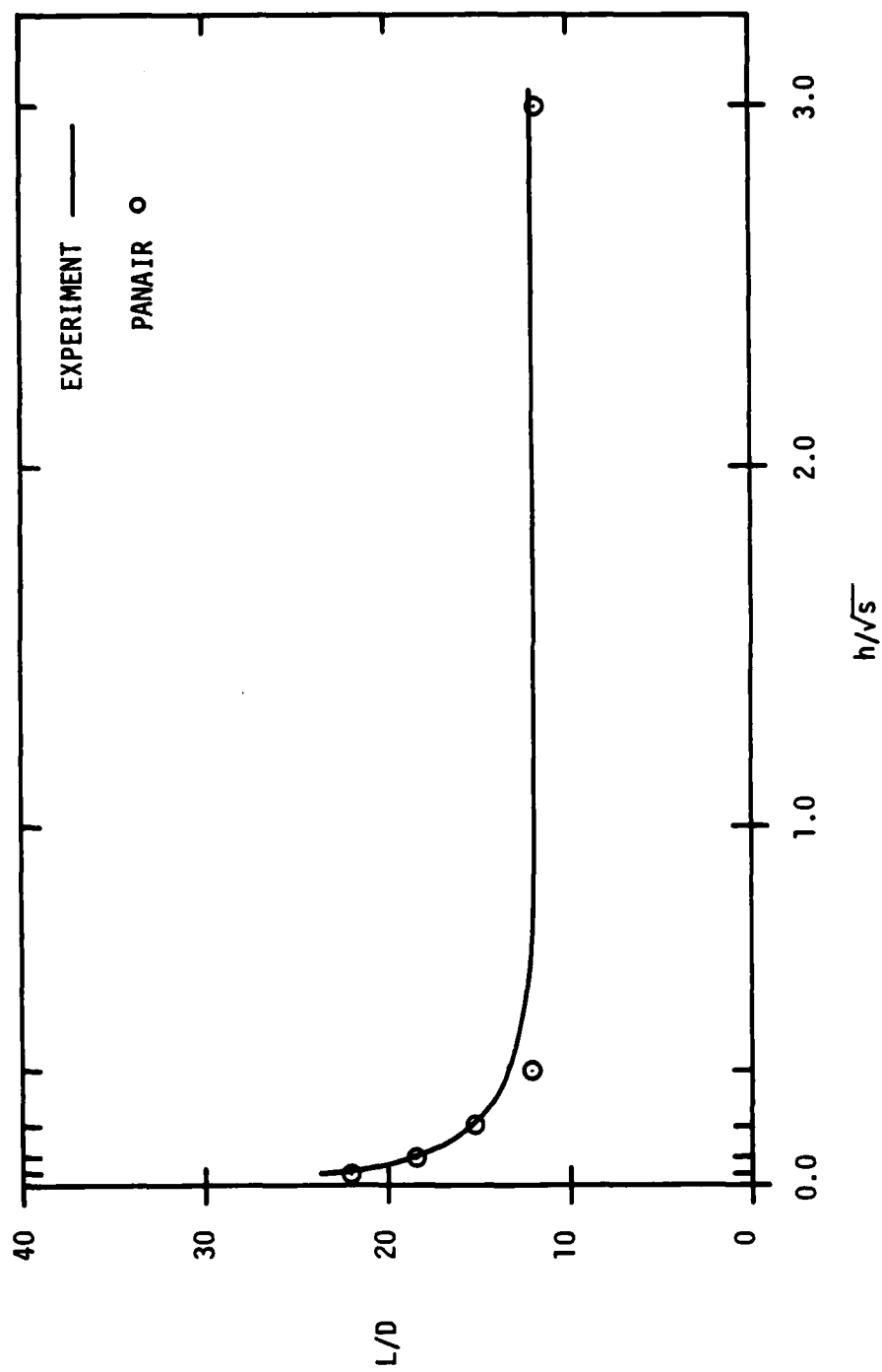


Figure 13.  $L/D$  vs  $h/\sqrt{s}$  Without Endplates,  $\alpha = 2^\circ$

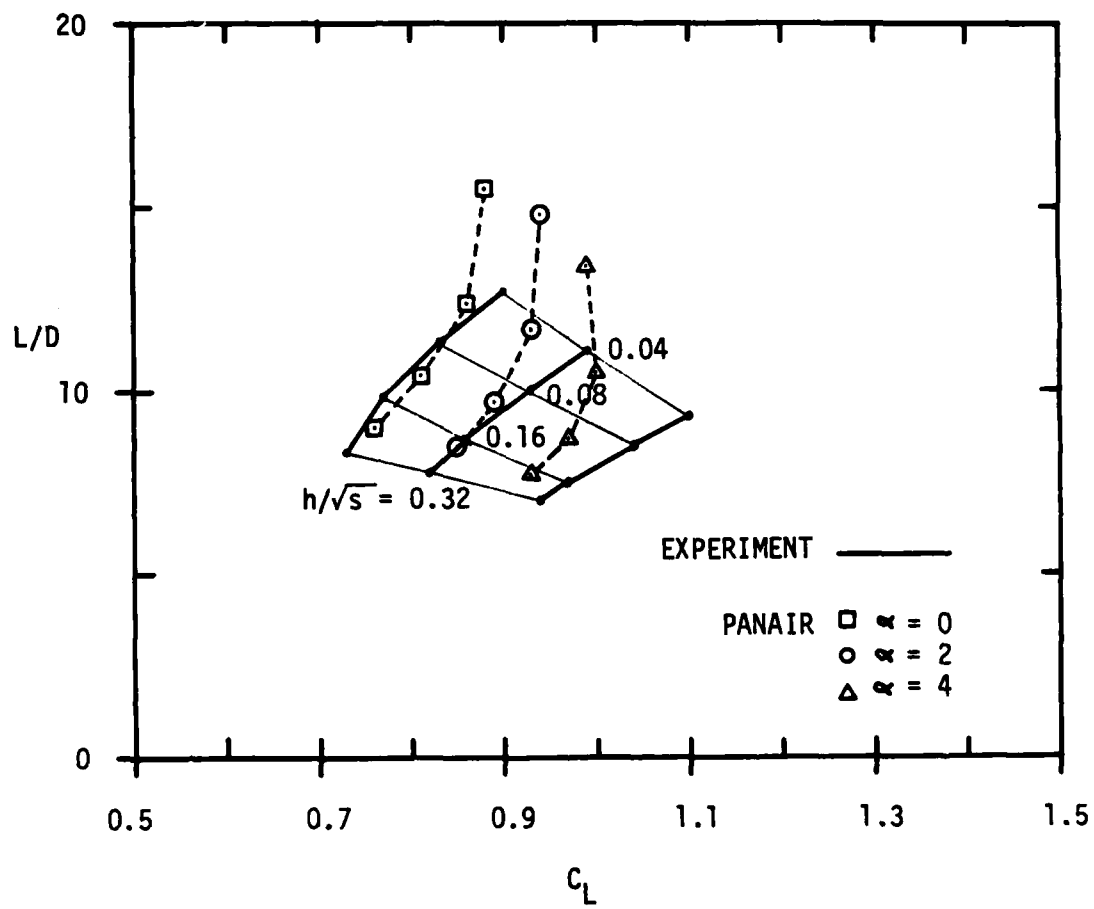


Figure 14. L/D Comparison Without Endplates,  
Flap Deflection = 15°

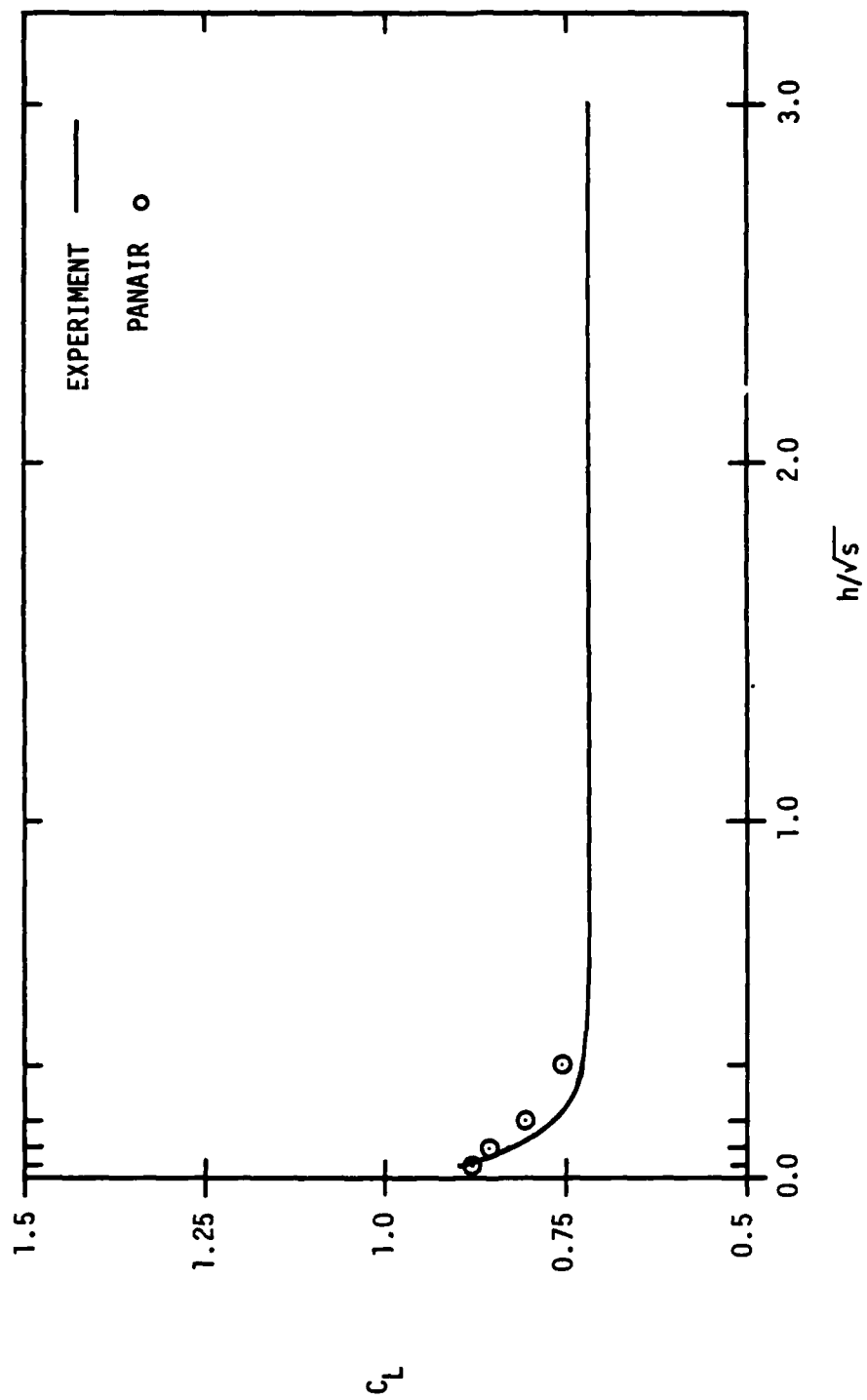


Figure 15.  $C_L$  vs.  $h/\sqrt{s}$  Without Endplates,  $\alpha = 0^\circ$

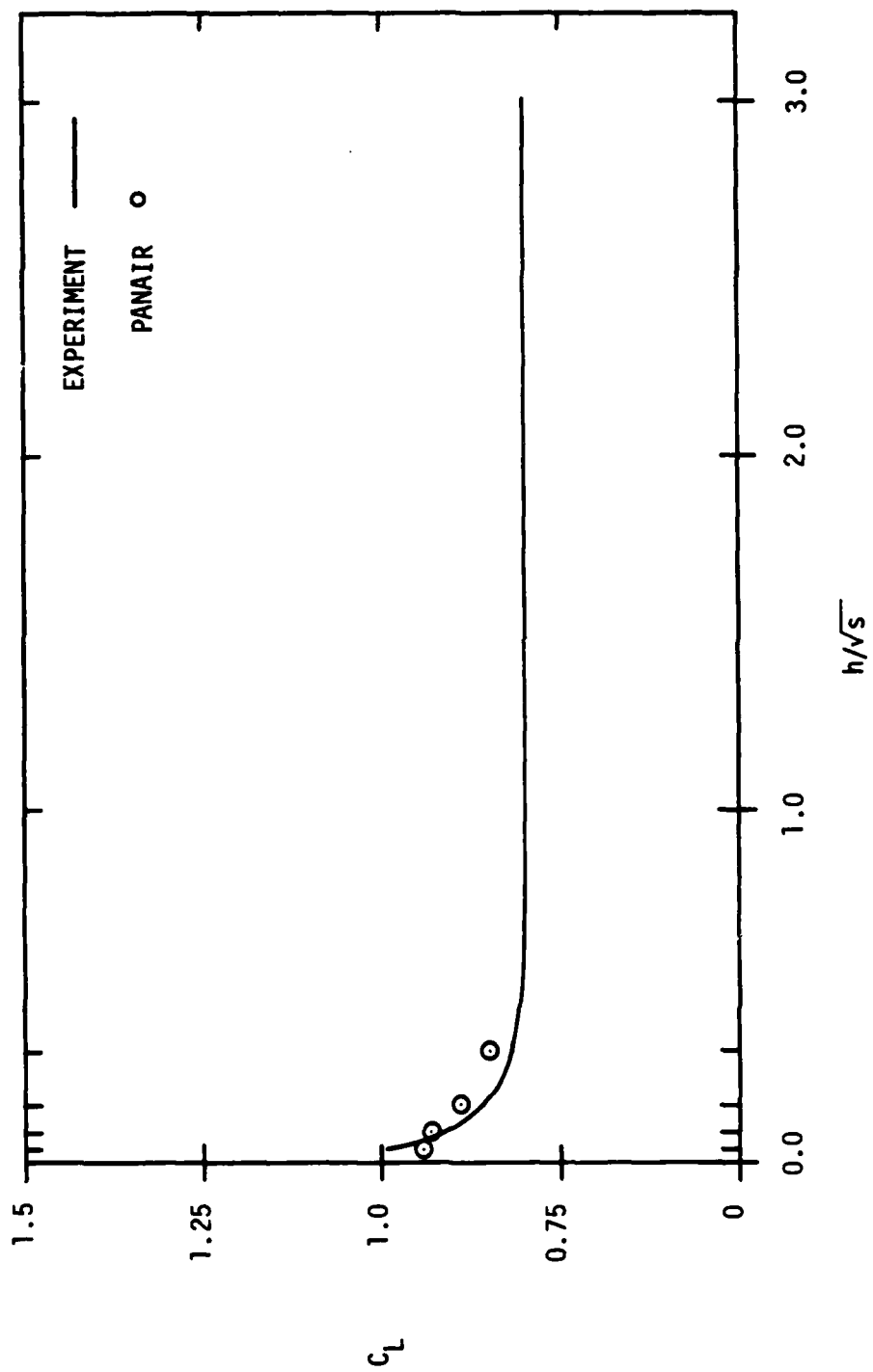


Figure 16.  $C_L$  vs.  $h/\sqrt{s}$  Without Endplates,  $\alpha = 2^\circ$

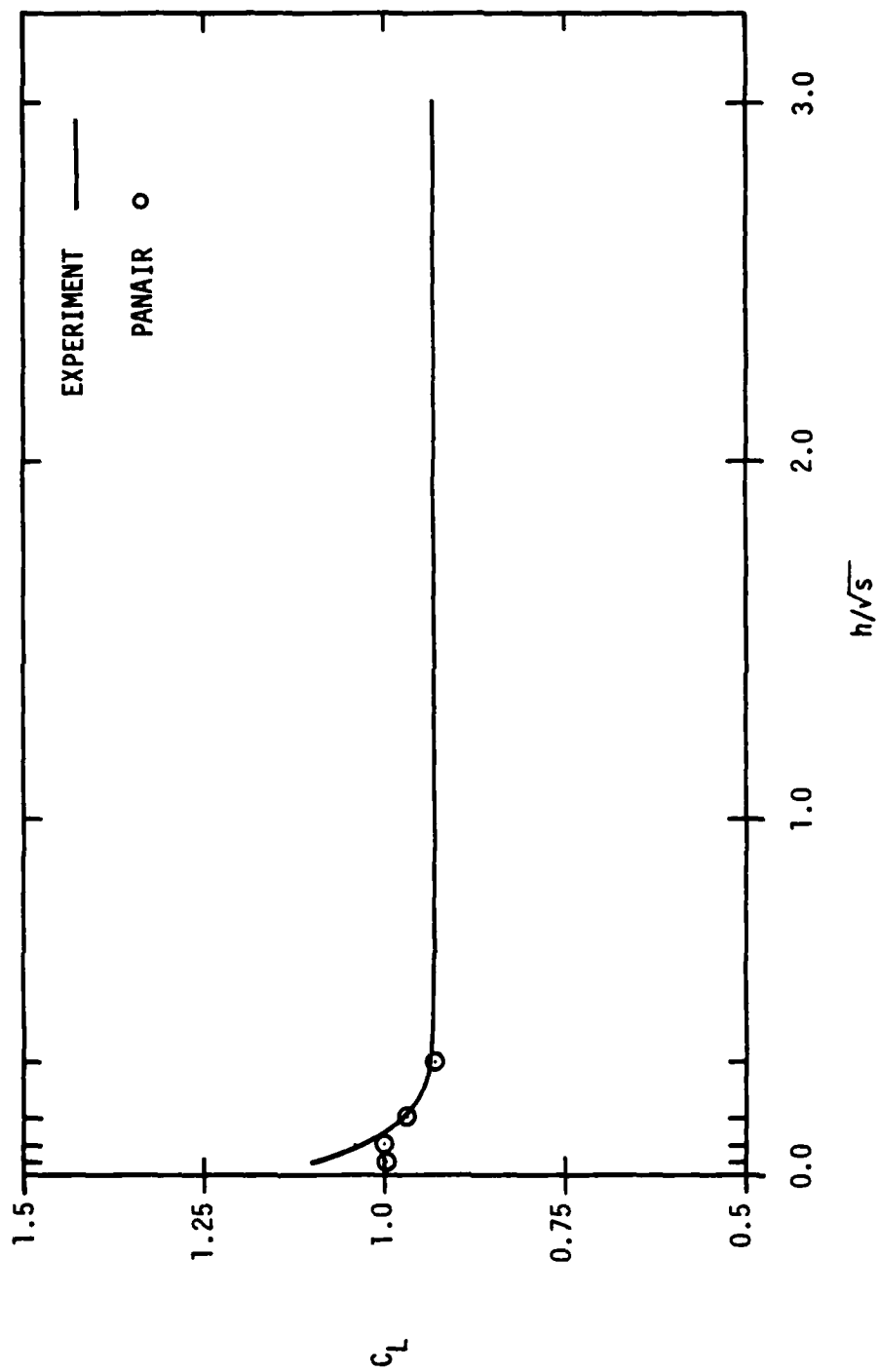


Figure 17.  $C_L$  vs.  $h/\sqrt{s}$  Without Endplates,  $\alpha = 4^\circ$

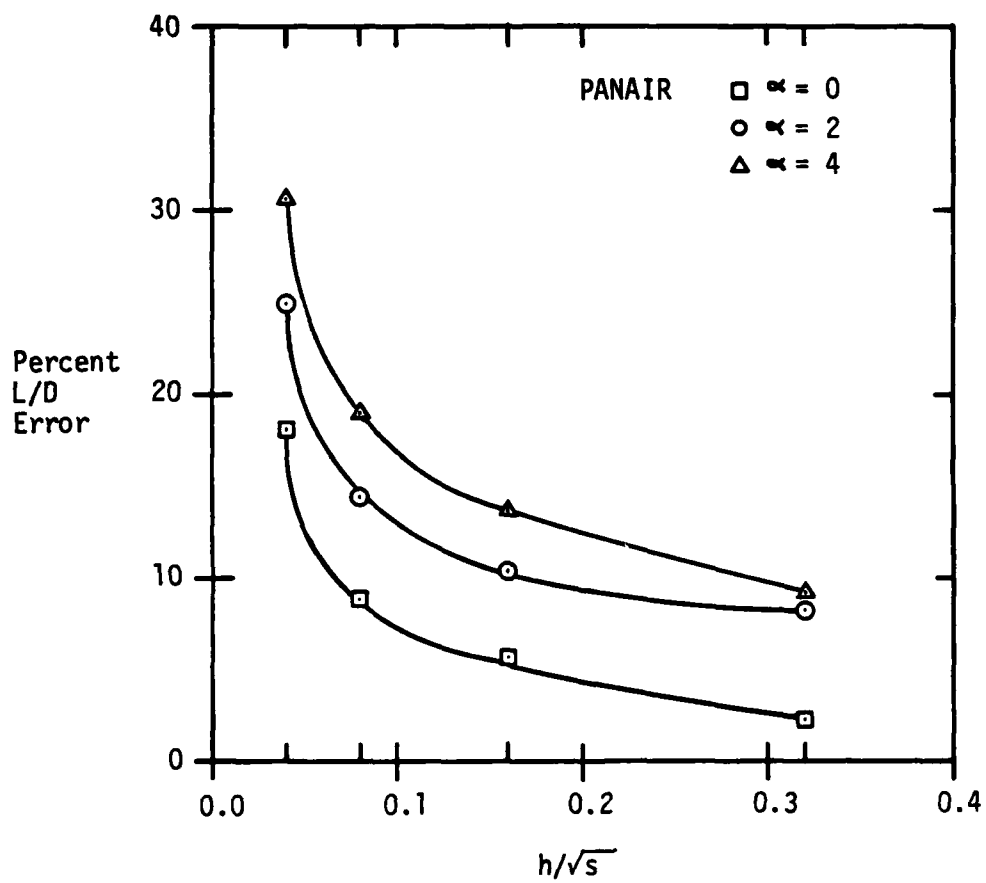


Figure 18. Percent L/D Error vs.  $h/\sqrt{s}$  Without Endplates, Flap Deflection =  $15^\circ$

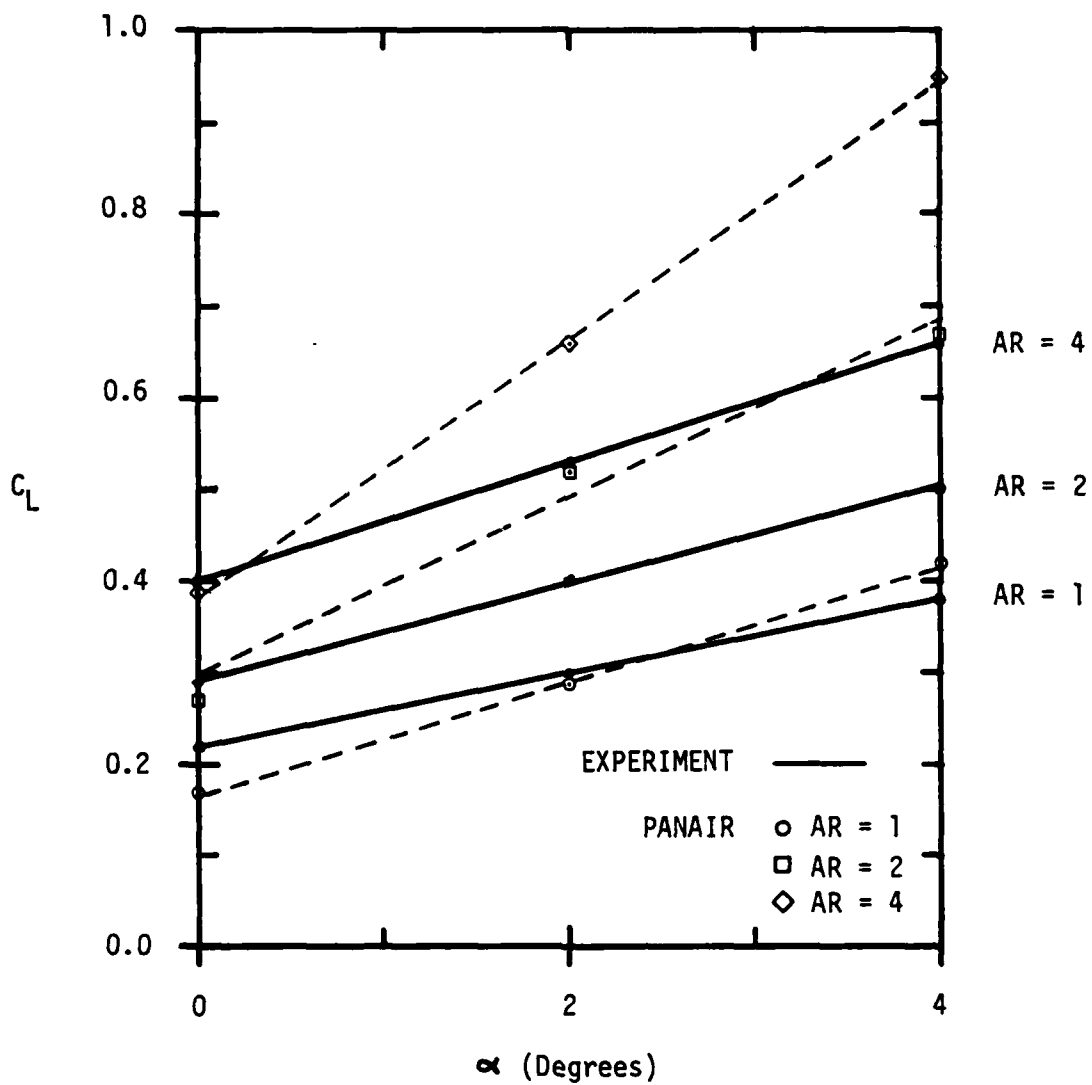


Figure 19. Lift Curve Slope With Endplates,  
Flap Deflection =  $0^\circ$

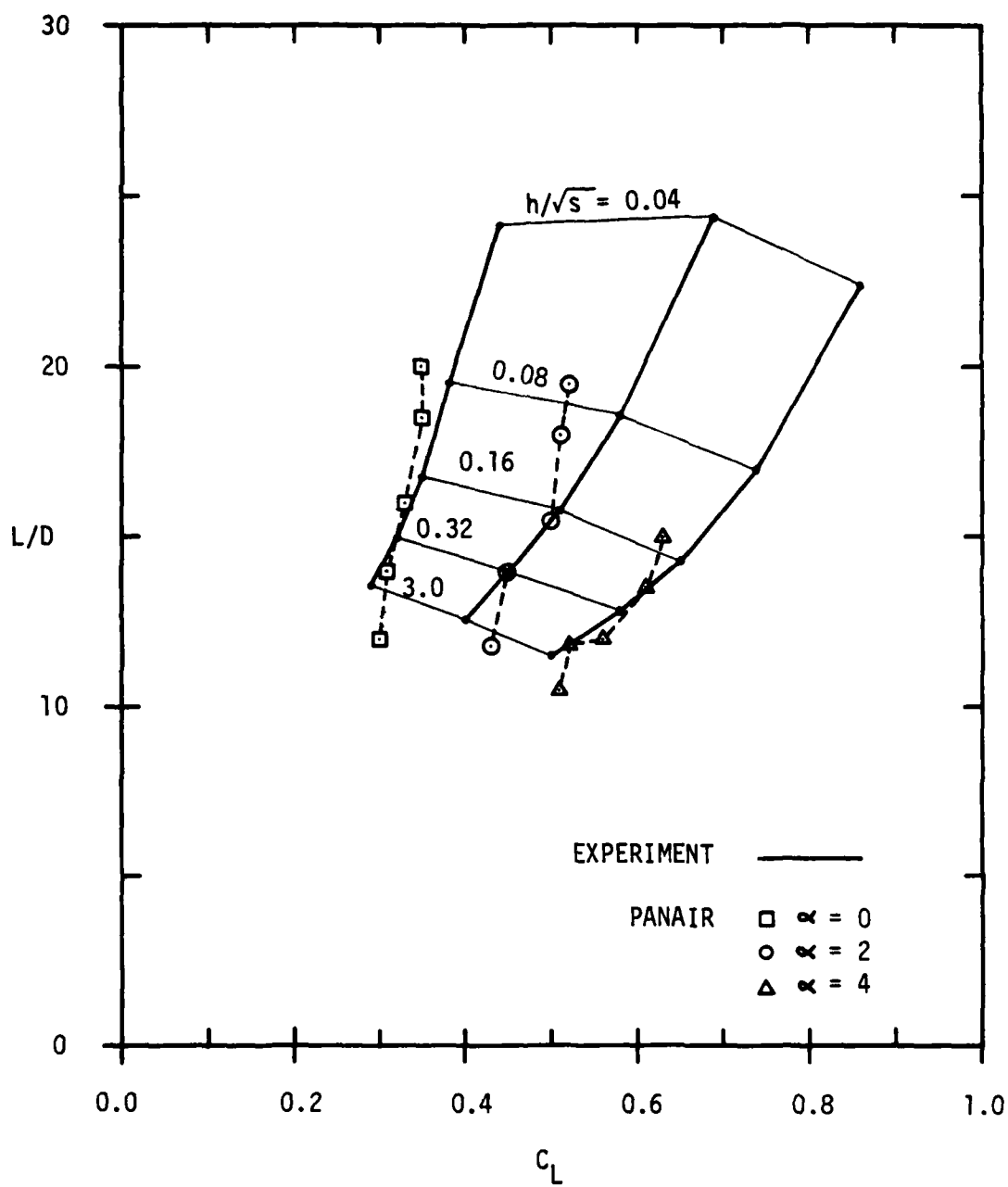


Figure 20. L/D Comparison With Endplates,  
Flap Deflection = 0°

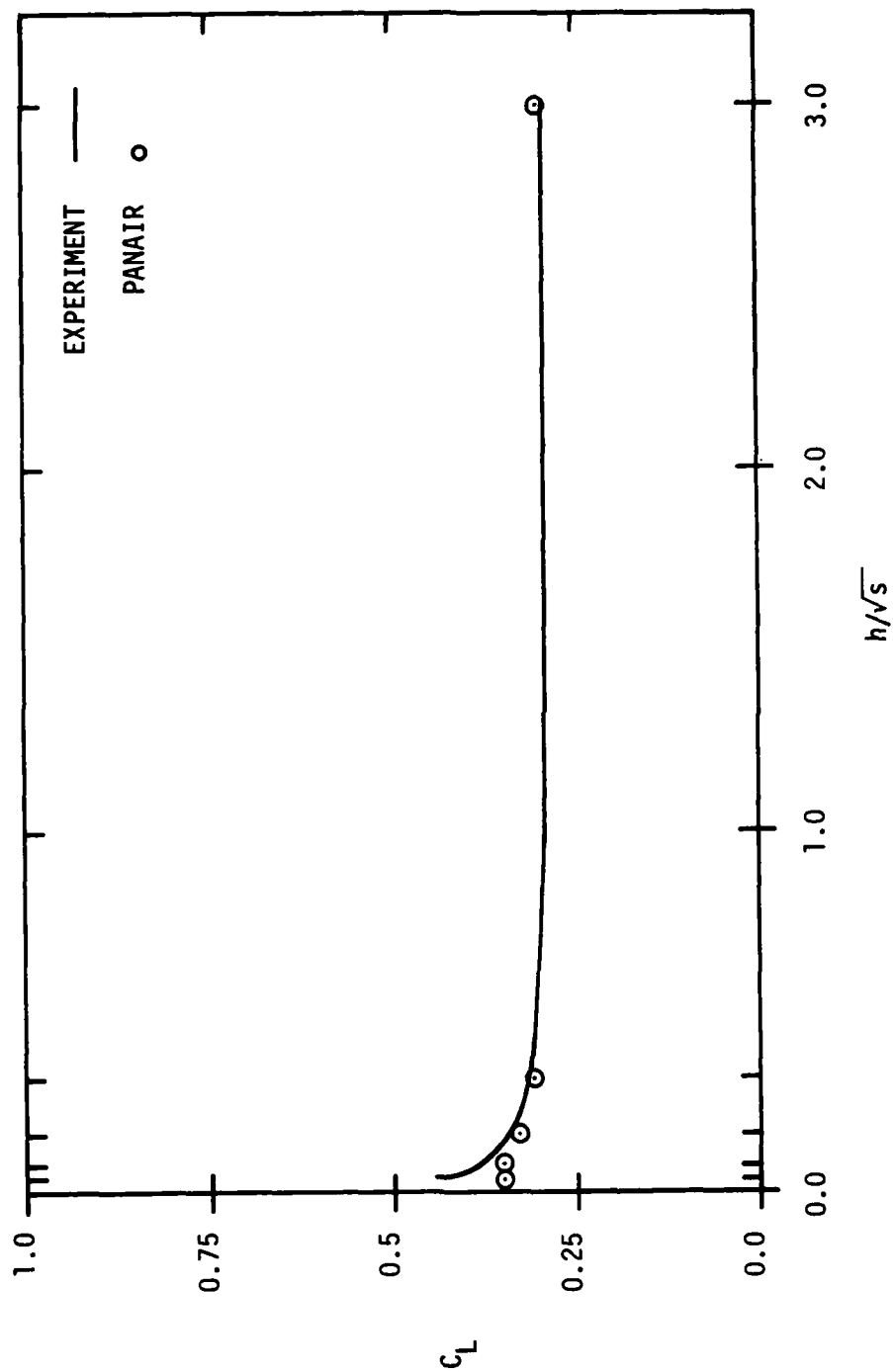


Figure 21.  $C_L$  vs.  $h/\sqrt{s}$  With Endplates,  $\alpha = 0^\circ$

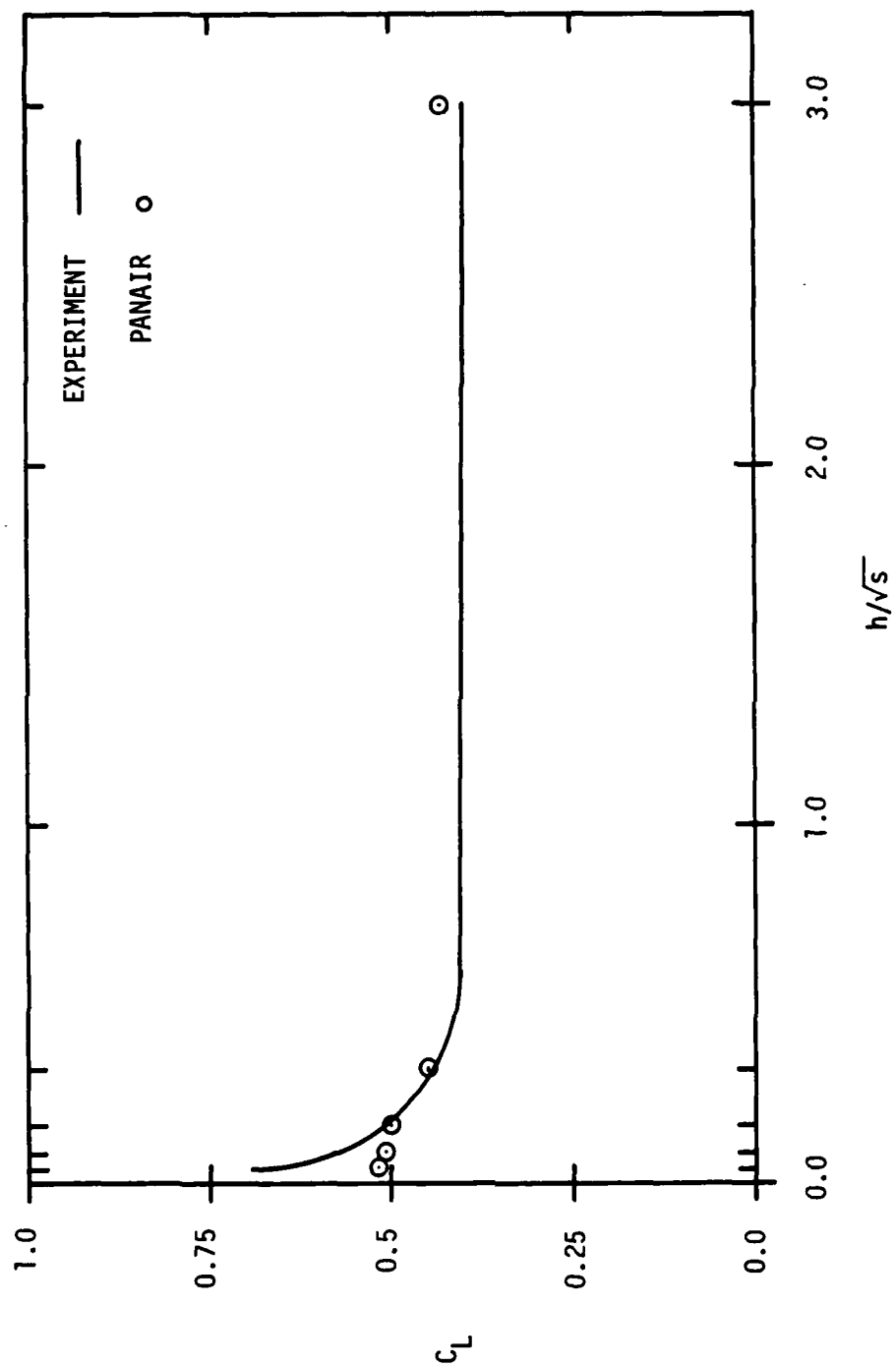


Figure 22.  $C_L$  vs.  $h/\sqrt{s}$  With Endplates,  $\alpha = 2^\circ$

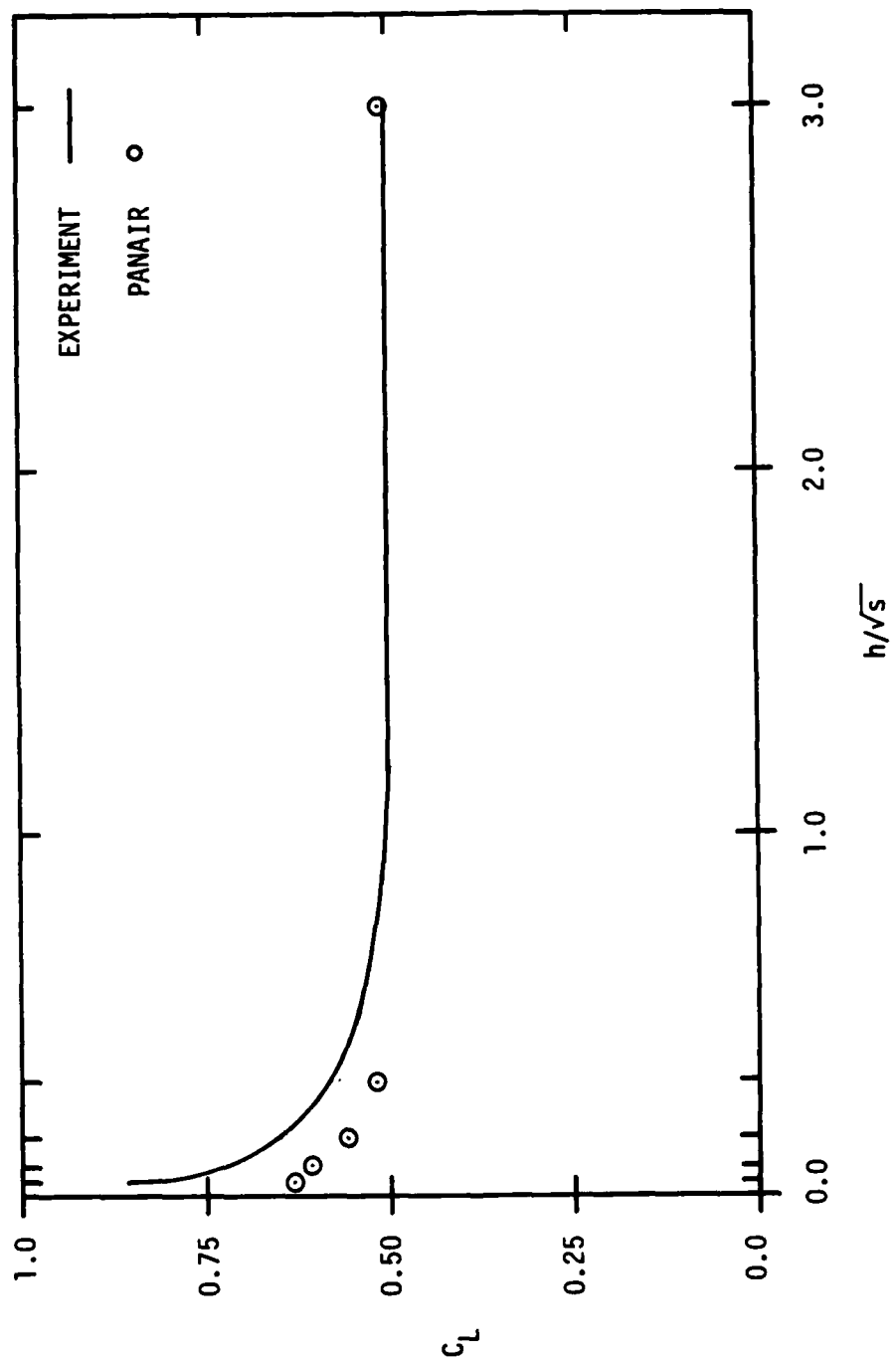


Figure 23.  $C_L$  vs.  $h/\sqrt{s}$  With Endplates,  $\alpha = 4^\circ$

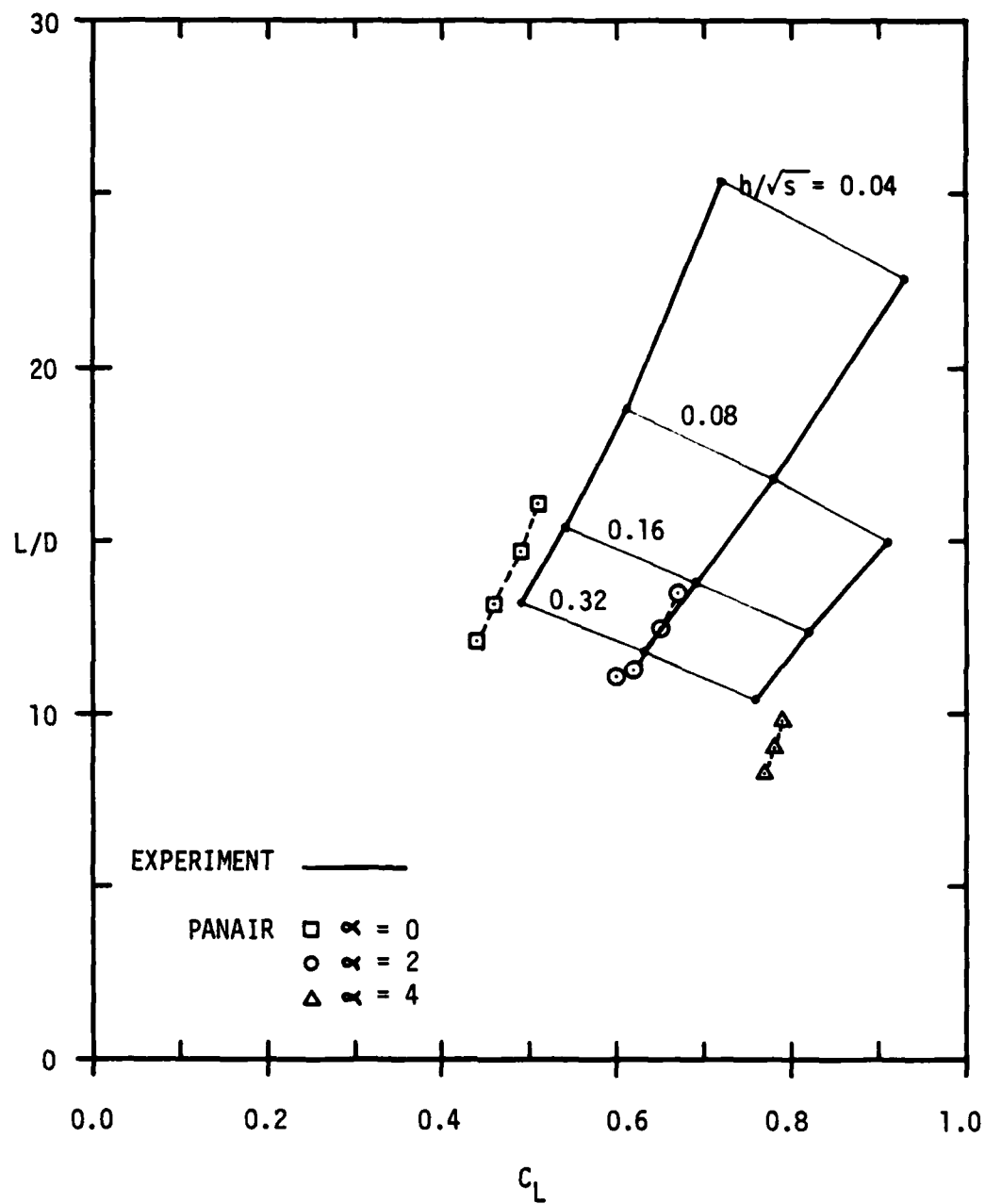


Figure 24.  $L/D$  Comparison With Endplates,  
Flap Deflection =  $5^\circ$

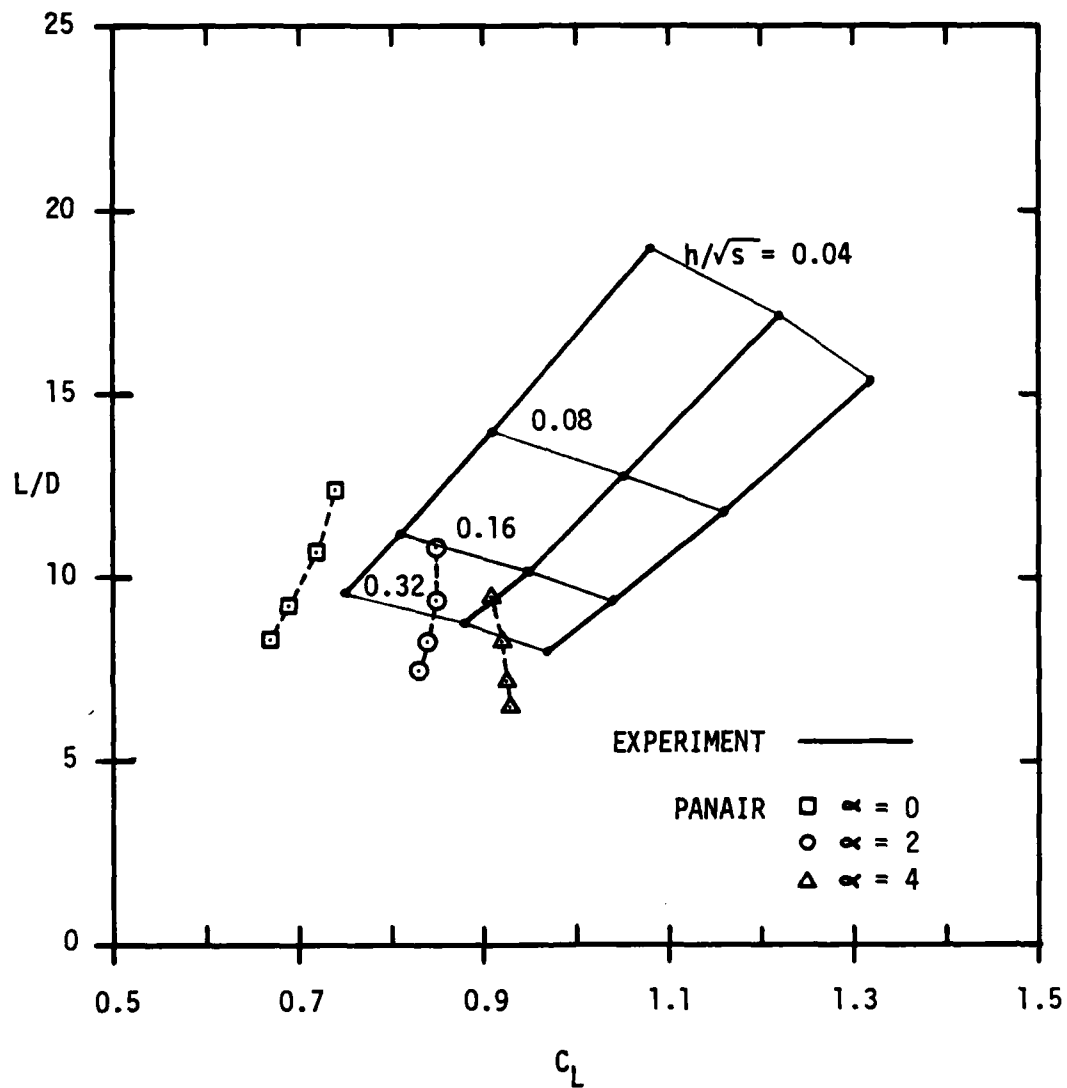


Figure 25.  $L/D$  Comparison With Endplates,  
Flap Deflection =  $15^\circ$

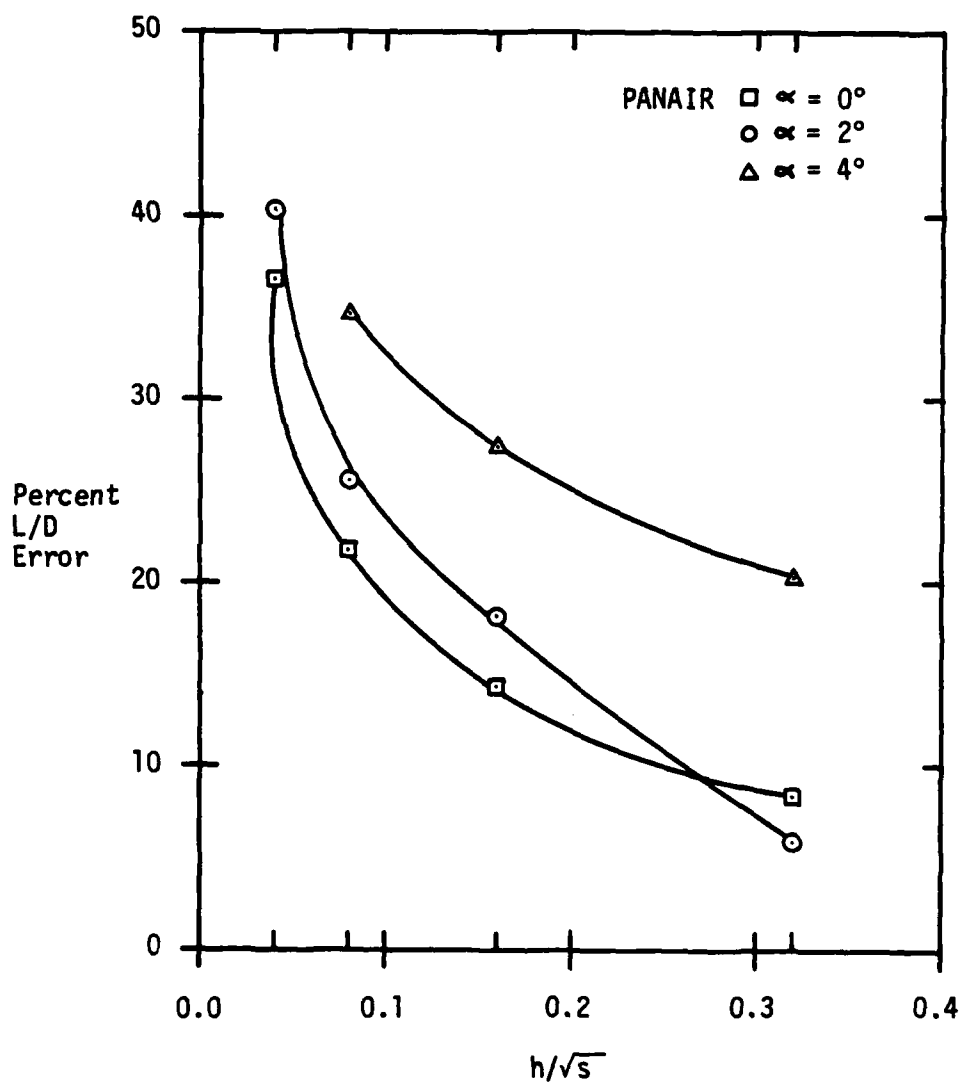


Figure 26. Percent L/D Error vs.  $h/\sqrt{s}$  With Endplates, Flap Deflection =  $5^\circ$

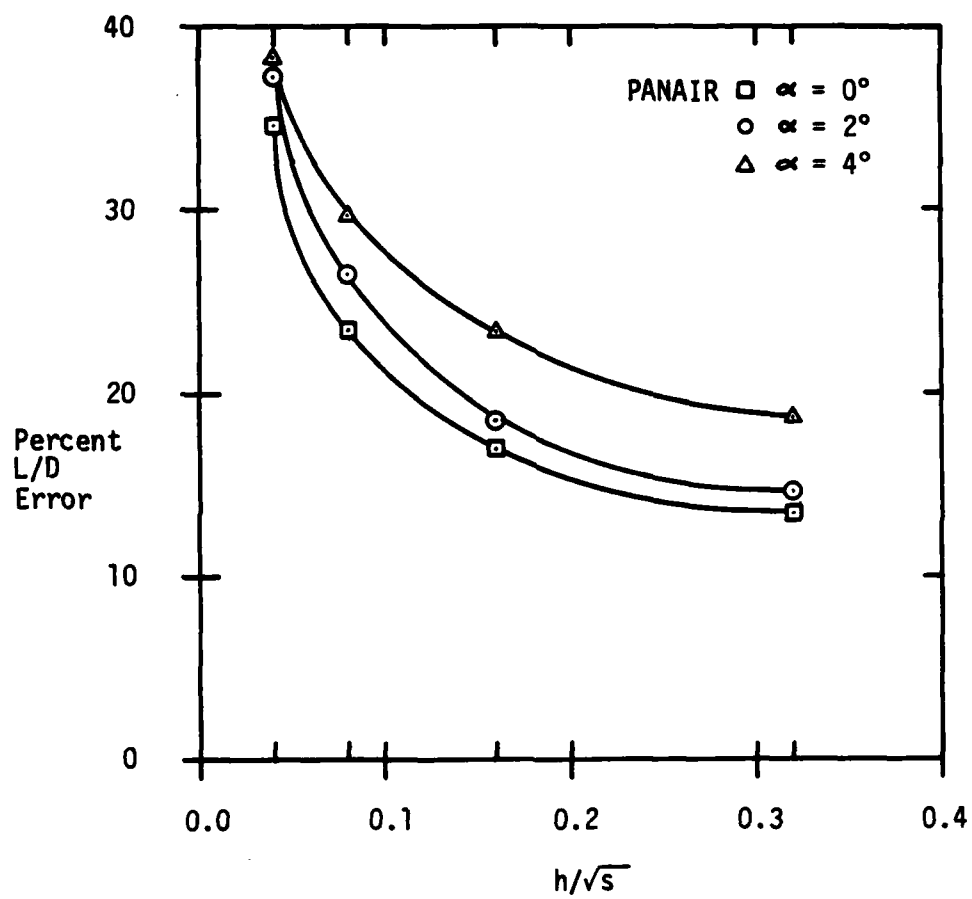


Figure 27. Percent L/D Error vs.  $h/\sqrt{s}$  With Endplates, Flap Deflection =  $15^\circ$

Appendix: WIG Configurations Examined

Without Endplates

<u>Angle of Attack (Degrees)</u>	<u>Flap Deflection (Degrees)</u>	<u><math>h/\sqrt{s}</math></u>	<u>Aspect Ratio</u>
0.0	0.0	3.0	1.0
2.0	0.0	3.0	1.0
4.0	0.0	3.0	1.0
0.0	0.0	3.0	2.0
0.0	0.0	0.32	2.0
0.0	0.0	0.16	2.0
0.0	0.0	0.08	2.0
0.0	0.0	0.04	2.0
2.0	0.0	3.0	2.0
2.0	0.0	0.32	2.0
2.0	0.0	0.16	2.0
2.0	0.0	0.08	2.0
2.0	0.0	0.04	2.0
0.0	0.0	3.0	4.0
2.0	0.0	3.0	4.0
4.0	0.0	3.0	4.0
0.0	15.0	0.32	2.0
0.0	15.0	0.16	2.0
0.0	15.0	0.08	2.0
0.0	15.0	0.04	2.0

<u>Angle of Attack (Degrees)</u>	<u>Flap Deflection (Degrees)</u>	<u><math>h/\sqrt{s}</math></u>	<u>Aspect Ratio</u>
2.0	15.0	0.32	2.0
2.0	15.0	0.16	2.0
2.0	15.0	0.08	2.0
2.0	15.0	0.04	2.0
4.0	15.0	0.32	2.0
4.0	15.0	0.16	2.0
4.0	15.0	0.08	2.0
4.0	15.0	0.04	2.0

With Endplates

0.0	0.0	3.0	1.0
2.0	0.0	3.0	1.0
4.0	0.0	3.0	1.0
0.0	0.0	3.0	2.0
0.0	0.0	0.32	2.0
0.0	0.0	0.16	2.0
0.0	0.0	0.08	2.0
0.0	0.0	0.04	2.0
2.0	0.0	3.0	2.0
2.0	0.0	0.32	2.0
2.0	0.0	0.16	2.0
2.0	0.0	0.08	2.0
2.0	0.0	0.04	2.0

<u>Angle of Attack (Degrees)</u>	<u>Flap Deflection (Degrees)</u>	<u><math>h/\sqrt{s}</math></u>	<u>Aspect Ratio</u>
4.0	0.0	3.0	2.0
4.0	0.0	0.32	2.0
4.0	0.0	0.16	2.0
4.0	0.0	0.08	2.0
4.0	0.0	0.04	2.0
0.0	0.0	3.0	4.0
2.0	0.0	3.0	4.0
4.0	0.0	3.0	4.0
0.0	5.0	0.32	2.0
0.0	5.0	0.16	2.0
0.0	5.0	0.08	2.0
0.0	5.0	0.04	2.0
2.0	5.0	0.32	2.0
2.0	5.0	0.16	2.0
2.0	5.0	0.08	2.0
2.0	5.0	0.04	2.0
4.0	5.0	0.32	2.0
4.0	5.0	0.16	2.0
4.0	5.0	0.08	2.0

<u>Angle of Attack (Degrees)</u>	<u>Flap Deflection (Degrees)</u>	<u><math>h/\sqrt{s}</math></u>	<u>Aspect Ratio</u>
0.0	15.0	0.32	2.0
0.0	15.0	0.16	2.0
0.0	15.0	0.08	2.0
0.0	15.0	0.04	2.0
2.0	15.0	0.32	2.0
2.0	15.0	0.16	2.0
2.0	15.0	0.08	2.0
2.0	15.0	0.04	2.0
4.0	15.0	0.32	2.0
4.0	15.0	0.16	2.0
4.0	15.0	0.08	2.0
4.0	15.0	0.04	2.0

### Bibliography

1. Sidewell, J. R., Baruah, P. K., and Bussoletti, J.E. PANAIR-A Computer Program for Predicting Subsonic or Supersonic Linear Potential Flows About Arbitrary Configurations Using a Higher Order Panel Method. NASA CR3252, May 1980.
2. Brown, J. R. Wind Tunnel Investigation of Single and Tandem Low Aspect Ratio Wings in Ground Effect. TRECOM TR-63-63, March 1964.
3. Miller, S. G., Youngblood, D. B. Applications of USSAERO-B and the PANAIR Production Code to the CDAF Model A Canard/Wing Configuration. AIAA-83-1829, July 1983.
4. Thwaites, B. Fluid Motion Memoirs--Incompressible Aerodynamics--An Account of the Theory and Observation of the Steady Flow of Incompressible Fluid Past Aerofoils, Wings and Other Bodies. Oxford: University Press, 1960.
5. Jones, B. Elements of Practical Aerodynamics (Fourth edition). New York: John Wiley & Sons, Inc., 1950.
6. Carter, A. W. Effect of Ground Proximity on the Aerodynamic Characteristics of Aspect Ratio 1 Airfoils With and Without End Plates. NASA TN D-970, October 1961.
7. Wieselsberger, C. Wing Resistance Near the Ground. NACA TM 77, 1922.
8. Serebrisky, Y. M., Biachuev, S. A. Wind Tunnel Investigation of the Horizontal Motion of a Wing Near the Ground. NACA TM 1095, 1946.
9. Waskiewicz, J. E., DeJough, J., and Cenko, A. Application of Panel Methods to the Aerodynamic Analysis of Proximity and Mutual Interference Effects on Store Separation at Supersonic Speeds. AIAA-83-0009, January 1983.
10. DeHart, J. H., Kramer, K. R., and Miller, S. G. Application of the PANAIR Production Code to a Complex Canard Wing Configuration. AIAA-83-0009, January 1983.
11. Haake, M., Kleinedam, G. Flight-Mechanical and Aerodynamic Investigations With Regard to the Ram-Wing Concept. BMVg-FBWT 79-4, August 1979.
12. Gallington, R. W., Miller, M. K., and Smith, W. D. The Ram-Wing Surface Effect Vehicle: Comparison of One-Dimensional Theory With Wind Tunnel and Free Flight Results. SRL-TR-71-0012, July 1971.

## VITA

Alfred R. Goetz was born on 3 February 1959 in Pittsburgh, Pennsylvania. He graduated from high school in Pittsburgh in 1977 and attended the University of Pittsburgh from which he received the degree of Bachelor of Science in Mechanical Engineering in April 1981. Upon graduation, he obtained employment as an aerospace engineer at the Foreign Technology Division at Wright-Patterson AFB, Ohio. He entered the School of Engineering, Air Force Institute of Technology, in October 1981 as a part-time student.

Permanent Address: Apt. 122

251 W. Dayton Yellow-Springs Rd.

Fairborn, Ohio 45324

UNCLASSIFIED

SECURITY CLASSIFICATION OF THIS PAGE

## REPORT DOCUMENTATION PAGE

1a. REPORT SECURITY CLASSIFICATION Unclassified			1b. RESTRICTIVE MARKINGS		
2a. SECURITY CLASSIFICATION AUTHORITY			3. DISTRIBUTION/AVAILABILITY OF REPORT Approved for public release; Distribution unlimited.		
2b. DECLASSIFICATION/DOWNGRADING SCHEDULE					
4. PERFORMING ORGANIZATION REPORT NUMBER(S) AFIT/GAE/AA/84D-7			5. MONITORING ORGANIZATION REPORT NUMBER(S)		
6a. NAME OF PERFORMING ORGANIZATION School of Engineering Air Force Institute of Tech.		6b. OFFICE SYMBOL (If applicable) AFIT/EN	7a. NAME OF MONITORING ORGANIZATION		
6c. ADDRESS (City, State and ZIP Code) Wright-Patterson AFB, Ohio 45433			7b. ADDRESS (City, State and ZIP Code)		
8a. NAME OF FUNDING/SPONSORING ORGANIZATION Air Force Wright Aeronautical Laboratory		8b. OFFICE SYMBOL (If applicable) ArWAL/FIMM	9. PROCUREMENT INSTRUMENT IDENTIFICATION NUMBER		
8c. ADDRESS (City, State and ZIP Code) Wright-Patterson AFB, Ohio 45433			10. SOURCE OF FUNDING NOS.		
			PROGRAM ELEMENT NO.	PROJECT NO.	TASK NO.
11. TITLE (Include Security Classification) See Box 19			WORK UNIT NO.		
12. PERSONAL AUTHOR(S) Alfred R. Goetz, B.S.M.E.					
13a. TYPE OF REPORT MS Thesis		13b. TIME COVERED FROM _____ TO _____		14. DATE OF REPORT (Yr., Mo., Day) 1984 December	
				15. PAGE COUNT 67	
16. SUPPLEMENTARY NOTATION					
17. COSATI CODES			18. SUBJECT TERMS (Continue on reverse if necessary and identify by block number)		
FIELD	GROUP	SUB. GR.	Ground Effect, Fluid Dynamics, Aerodynamic Characteristics, Aspect Ratio		
20	04				
19. ABSTRACT (Continue on reverse if necessary and identify by block number)					
Title: AERODYNAMIC PERFORMANCE OF A WING IN GROUND EFFECT USING THE PANAIIR PROGRAM					
Thesis Advisor: Michael L. Smith, Lieutenant Colonel, USAF					
20. DISTRIBUTION/AVAILABILITY OF ABSTRACT UNCLASSIFIED/UNLIMITED <input checked="" type="checkbox"/> SAME AS RPT. <input type="checkbox"/> DTIC USERS <input type="checkbox"/>			21. ABSTRACT SECURITY CLASSIFICATION Unclassified		
22a. NAME OF RESPONSIBLE INDIVIDUAL Michael L. Smith, Lieutenant Colonel, USAF		22b. TELEPHONE NUMBER (Include Area Code) 513-255-2321		22c. OFFICE SYMBOL AFIT/CCE	

Approved for public release: IAW AFR 190-17.  
LYNN E. WILKINS  
Dean for Research and Professional Development  
Air Force Institute of Technology (AFIT)  
Wright-Patterson AFB OH 45433

UNCLASSIFIED

SECURITY CLASSIFICATION OF THIS PAGE

The primary objective of this study is to correlate computed theoretical data with experimental data for wings in ground effect. This investigation uses the PANAIR higher-order panel method to predict the lift and drag characteristics of an aspect ratio two wing, with and without endplates, operating at low speed in ground effect. The effects of altitude, trailing edge flap deflection and angle of attack are considered. Numerical results are compared with subsonic wind tunnel experimental data. For both the numerical and experimental methods, the image model technique is used to simulate ground effect. Excellent agreement between numerical results and experimental data is achieved for the wing without endplates down to low (approximately ten percent of wing chord) altitudes. For the wing with endplates, numerical results are in good agreement with the experimental data for altitudes greater than approximately twenty percent of the wing chord. PANAIR results diverged from experimental data at lower altitudes because the model did not attempt to account for spanwise flow between the bottom of the endplate and the ground, and other viscous effects which tend to become dominant. These include a static pressure increase beneath the wing and wake distortions behind the configuration.

UNCLASSIFIED

SECURITY CLASSIFICATION OF THIS PAGE

**END**

**FILMED**

**5-85**

**DTIC**